Report of trilateral collaborative study among Japan, Korea and Taiwan for producing joint abundance indices for the yellowfin tunas in the Indian Ocean using longline fisheries data up to 2019

Toshihide Kitakado[1], Sheng-Ping Wang[2], Keisuke Satoh[3], Sung Il Lee[4], Wen-Pei Tsai[5], Takayuki Matsumoto[6], Hiroki Yokoi[3], Kei Okamoto[6], Mi Kyung Lee[4], Jung-Hyun Lim[4], Youjung Kwon[4], Nan-Jay Su[2], Su-Ting Chang[7] and Feng-Chen Chang[7]

[1] Tokyo University of Marine Science and Technology, 5-7, Konan 4, Minato, Tokyo, 108-8477, Japan (Email: kitakado@kaiyodai.ac.jp)

[2] National Taiwan Ocean University, No. 2, Beining Rd., Zhongzheng Dist., Keelung City 20224, Taiwan

[3] National Research and Development Agency, Japan Fisheries Research and Education Agency, Fisheries Resources Institute, 2-12-4 Fukuura, Kanazawa-ku, Yokohama-shi, kanagawa-ken, 236-8648, JAPAN

[4] National Institute of Fisheries Science, 216 Gijanghaean-ro, Gijang-eup, Gijang-gun, 46083 Busan, Korea

[5] National Kaohsiung University of Science and Technology, No. 415, Jiangong Rd., Sanmin Dist., Kaohsiung City 80778, Taiwan

[6] National Research and Development Agency, Japan Fisheries Research and Education Agency, Fisheries Resources Institute, 5-7-1, Orido, Shimizu, Shizuoka-shi, 424-8633, Japan

[7] Overseas Fisheries Development Council, 3F., No.14, Wenzhou St., Da'an Dist., Taipei City 10648, Taiwan

ABSTRACT

Three distant-water tuna longline countries, Japan, Korea and Taiwan, have started a collaborative study since December 2019 for producing the joint abundance indices using integrated fishery data of these fleets to contribute to the upcoming stock assessments of yellowfin tuna in the Indian Ocean. The intention is to produce reliable indices by increasing the spatial and temporal coverage of fishery data. In this paper, some preliminary results using data up to 2019 fisheries were provided to update the WPTT on the progress of this activity.

As an underlying analysis, a clustering approach was utilized to account for the inter-annual changes of the target in each fishery in each region. Due to high dimensionality of fishery data with species composition, a two-step procedure was employed. A "K-means clustering" method with a pre-specified large number of initial clusters was firstly applied to fine scale fishery data in order to reduce the dimension of data, and then the aggregated data based on the first step were used in the subsequent "hierarchical clustering". The whole process was repeated through a certain number of iterations with different random initial clusters to seek a set of the smallest sum of within-cluster variation. The outputs of the finalized cluster were then used to assign the cluster label on fishery target to each catch-effort data.

For standardizing the catch-per-unit-effort data, the conventional linear models and delta-lognormal linear models were employed for data of monthly and 1° grid resolution in each region. In addition to the implicit target species through the clustering, geographical and temporal covariates were used in the regression structures. The models were diagnosed by the standard residual plots and influence analysis. Although the results shown in this paper were still preliminary because of a delay and difficulty in the data-sharing process, a final set of results based on the updated data including 2020 fishery outcomes will be submitted before the upcoming yellowfin tuna stock assessment meeting scheduled in October 2021 for use as inputs for the update of its stock assessment.

Besides these conventional regression methods, analyses using an advanced spatio-temporal model, vector-autoregressive spatio-temporal model (VAST), were attempted for developing abundance indices with additional consideration of spatio-temporal correlations and targets as well as the life stage of yellowfin tuna. In the VAST analysis, the convergence was not achieved enough when aggregating the three fisheries data yet, but the codes were developed well and ready to use for the finalization of results.

As other future works, the regional scaling will be applied for the conventional regression models so that a constant catchability can be assumed across the regions in the stock assessment models. The regional trends in the standardized CPUE are then compared to those from the VAST analysis, where catchability is constant by default and the regional scaling is not required.

INTRODUCTION

Tuna-RFMOs, including the IOTC, recommended that the joint CPUE of longline fisheries be developed to improve the stock assessments for tropical tunas, and thus the IOTC has conducted collaborative works for several years to produce an abundance index by combining CPUEs data from major longline fleets. An ensemble approach of fishery data from multiple longline fleets has been applied to the tropical and temperate tuna species for their stock assessments (e.g. Hoyle et al. 2018, Hoyle et al. 2019a, 2019b).

However, it was found that the fishing technologies, data formats, spatial-temporal coverage were different among the fleets, and therefore it is important to discuss and exchange the information among countries using ample time in order to improve the analysis and index. To this end, three longline countries, Japan, Korea and Taiwan, have been conducting a collaborative study for developing the abundance index since December 2019. In this paper, some preliminary results using data up to 2019 fisheries were provided to update the WPTT on the progress of this activity.

MATERIALS

Data sharing protocol

Initially, the analysis was planned to conduct in a series of in-person meetings through data sharing in an intranet system to ensure the data security. However, after a face-to-face meeting in Busan in December 2019, we have been holding only webinar meetings (a total of 15 times until April 2021) because of COVID-19 pandemic. Under this circumstance, a data sharing protocol was finalized among the three countries with a restriction of data access only by the Chair of the group (Toshihide Kitakado) for reduced resolution of data set (not operational data but some aggregated data over 1° square grid by month by vessel).

Figures 1 represents distributions of fishing efforts by decade for longline fisheries of three countries. Their annual nominal CPUEs and mean length of yellowfin tuna in the IOTC convention area are also shown in Figures 2 and 3, respectively, based on the regional definition shown in Figure 4.

The data set combined for yellowfin CPUE standardization were available from 1975 to 2019, with data fields of year and month of operation, location to 1° of latitude and longitude, vessel id, number of hooks, and catch by species in number. We classified the species into albacore (ALB), bigeye (BET), yellowfin (YFT), Indian bluefin tuna (BFT), southern bluefin tuna (SBT), black marlin (BLM), blue marlin (BUM), swordfish (SWO), other billfishes (BIL), sharks (SKX) and others (OTH).

METHODS

Analytical procedures (including planned works)

For standardizing the catch-per-unit-effort data, the conventional linear models and delta-lognormal linear models were employed for data of monthly and 1° grid resolution in each region. In addition to the implicit target species through the clustering, geographical and temporal covariates were used in the regression structures. The models were diagnosed by the standard residual plots and influence analysis and compared via the model selection criteria. Besides these conventional regression methods, analyses using an advanced spatio-temporal model, VAST, were attempted for developing abundance indices with additional consideration of spatio-temporal correlations and targets as well as the life stage of yellowfin tuna. So, in a nutshell, the approaches are as follows:

1) investigation of better approaches to account for changes in targeting within each country;

2) analyses using conventional regression models (e.g. delta-lognormal model) with geographical, environmental and fishery (including targeting) information for continuity from the previous approaches; and

3) analysis using an advanced spatio-temporal model (VAST) for developing abundance indices with additional consideration of spatio-temporal correlations and size structure.

Cluster analysis

Overview

As an underlying analysis, a clustering approach was utilized to account for the inter-annual changes of the target in each fishery in each region. Due to high dimensionality of fishery data with species composition, a two-step procedure proposed by He et al. (1997) was employed. A "K-means clustering" method with a pre-specified enough large number of initial clusters (say *K*, the argument "centers" in "kmeans" of R function) and a chosen random set (the argument "nstart" in "kmeans" of R function) was firstly applied to fine scale fishery data in order to reduce the dimension of data, and then the aggregated data based on the first step were used in the subsequent "hierarchical clustering". In the previous analyses, K-means used to reduce the dimension was only performed for one iteration with low values of "centers" (${}_kP_2 \approx 40$ clusters; k is number of species) and "nstart", which may result in obviously inconsistent clustering results, especially for the dataset with catch composition consisted of mixture species. In the present analyses, the values of "centers" and "nstart" were increased for K-means and the whole process of two-step clustering was repeated through a certain number of iterations with different random seeds for K-means to seek an optimal set with the smallest sum of within-cluster variation obtained from hierarchical clustering. The outputs of the finalized cluster were then used to assign the cluster label fishery target to each catch-effort data.

Dataset

The dataset used for conducting the clustering consisted of *r* (the number of fishing set) x *c* (the number of species) data frame. For the Indian Ocean, albacore (ALB), bigeye tuna (BET), yellowfin tuna (YFT), swordfish (SWO), bluefin tuna (BFT), southern bluefin tuna (SBT) and sharks (SKX) were selected as main species and the catches of fishes other than these species were aggregated into a category of others (OTH). In addition, the data were aggregated by 10-days duration (1st-10th, 11th-20th, and 21st~ for each month) based on the agreement of the trilateral collaborative working group.

Specification of analysis (explanation of "distance" etc.)

For the K-means clustering, the trials with various values for the arguments of "centers" (from 40 to 1,000) and "nstart" (from 1 to 100) were tested. The values of "centers=500" and "nstart=30" were chosen since these settings can produce relatively robust results with less computation time for most datasets in different areas, but these values can be adjusted depending on the data.

For the hierarchical clustering, the trials with Ward's minimum variance and the complete linkage methods ("ward.D" and "complete" for the argument "method" in "hclust" of R function) applied to the squared Euclidean distances between data points calculated based on the species composition from the clusters of K-means were also conducted to examine the influence of agglomeration methods on the clustering results. Slight differences in the sum of within-cluster variations were observed from the results obtained using two agglomeration methods but may depend on the data from different areas. Therefore, Ward's minimum variance method, which is commonly used for conducting hierarchical clustering, was adopted for the present analyses. The number of clusters for the hierarchical cluster was determined when both the permutation ANOVA (PERMANOVA) for the centroids of the groups and the Beta diversity test permutation test for the homogeneity of multivariate dispersions achieve significances under the minimum number of clusters (Amruthnath and Gupta, 2019), and the improvement in the sum of within-cluster variations was less than 10%. Visualization diagnostics are also conducted based on the plots of centroids by clusters (boxplot and TukeyHSD) and plot from the principal coordinate analysis (PCoA) for the multivariate dispersions by clusters (Amruthnath and Gupta, 2019).

Selection of the final number of clusters

A total of 30 iterations were repeated for each set of two-step clustering process with different random seeds for K-means. The mode of the number of clusters obtained from 30 iterations was selected as the optimal number of clusters. Then the final outcome of the clustering was adopted based on the lowest value of the sum of within-cluster variation within the iterations with the optimal number of clusters.

Conventional regression analyses -LN and DL model-

Screening of data set

We eliminated data from some vessels, for which there were no catch records of yellowfin tuna in the study period. Also, we used data from vessels with at least 20 observations over all years, four quarters and all grids (explained below). Figure 5 shows empirical distributions of the vessel-wise number of data set in each region in each country. The vertical line is at a threshold of 20 used in this analysis. Figure 6 shows the time series of

positive probability rates in each region before and after applying the threshold value. As shown in this figure, proportions of 0-data are very low in all but Region 4. So, the conventional log-normal models might work for analyses in Region 2N, 2S, 3 and5, but there might be worth conducting the delta-type models in Region 4.

Log-normal (LN) regression models with a constant adjustment

Given that around 8.4% of the catch data are 0, we used an adjustment factor (here 10% of mean of CPUE) to the CPUE data to employ conventional log-normal distributions as follows:

$$log\ (CPUE + c) = Main\ effects + Interactions + Error$$

Potential covariates used in the analysis were shown below:

- Temporal component (year, month, quarter, year*quarter)
- Spatial component (5° squared longitudinal and latitudinal grid)
- Vessel ID
- Target (cluster outcomes to express target species of fishery)
- Number of hooks
- Interactions

The error terms are assumed to be independently and identically distributed as the normal distribution with mean 0 and standard deviation σ. The constant adjustment factor, c, is 10% of the overall mean as default.

Delta-lognormal (DL) regression model

A delta-lognormal model was also employed to account for "zero data" statistically as has been used in previous analyses (see e.g. Hoyle et al. 2018). For the first component of "zero" or "non-zero" is expressed as a binomial distribution with a probability of "non-zero" catch as a logistic relationship with some explanatory variables, and the second component for positive catch assumed the same regression structures used in the LN regression models with a constant adjustment.

Diagnosis and impacts of covariates (Residual plots, Q-Q plots, influence plots)

The standard residual plots were for the diagnosis for fitting of models to the data and Q-Q plots (only for the positive catch component in DL models). In addition, we used influence plots (Bentley et al. 2011) to interpret the contribution of each covariates to the difference between nominal and standardized temporal effects.

Extracts of abundance indices from models with interactions

Once the model fitting and model evaluation were conducted, the final output of the abundance index is extracted through an exercise of the least square means (so-called LS means) to account for heterogeneity of amount of data over covariate categories (as well as the standardized probability of "non-zero" catches in DL models).

Potential applications of regional scaling factors (concepts, models and interpretations)

Since we analyse the data by region to produce region-wise index, standardized CPUE series in different regions should have different catchability coefficients while that coefficient can be assumed to be common. However, the stock assessment integrates these CPUE series to produce a single and overall biomass and therefore it would be beneficial to produce another standardized CPUE, which can be directly comparable in terms of magnitude over regions. For this purpose, a method of regional scaling has been developed (Hoyle and Langley 2020). Here, due to a time constraint, we have not applied the method to our data formally, we will attempt the approach when updating the analysis with the finalized dataset including 2020 fishery data.

Spatial-temporal analyses (not conducted this time)

To express the spatial distribution, the generalized additive models (GAMs) tend to be useful, but it cannot deal with island/barrier/edge effects. The Gaussian Markov Random Field (GMRF) can account for them through triangulation of the domain with irregular shapes. Use of INLA is convenient for this process but it relies on

Bayesian framework. For the maximum likelihood estimation, use of Template Model Builder (TMB) is recommended after use of INLA only for triangulation because of availability of well-prepared approximation of stochastic partial differential equation (SPDE) function. In addition to the spatial component, the spatio-temporal auto-correlation helps to express inter-annual changes in the distribution patterns with use of philosophy of "borrowing strength" over space and time to draw information on density in space and time. These concepts have been achieved and implemented in the vector auto-regressive spatio-temporal (VAST) models with the advantage of faster computation with automatic differentiation and SPED approximation in the TMB.

We have used a package of VAST (Thorson and Barnett 2017; Thorson 2019). The spatial and temporal autocorrelations were incorporated in both of the delta and positive catch components. In addition, the difference in catchability over regions, fisheries and clusters was accounted in the model.

Regarding size specific VAST models, if the two datasets (logbook and size composition data) were aggregated in monthly intervals and 1° square grid, and then merged, which can be enable us to conduct the full time period analysis after 1975.

At the time of submission, there have been computational issues such as the convergence, and the authors have not yet gotten reasonable results. However, the work using actual data has just started, and therefore our efforts will be spent more before the upcoming yellowfin stock assessment meeting.

RESULTS

Cluster analysis

The results of cluster analysis were shown in Figure 7. In each country's analysis, the number of clusters ranged from 3 to 5, and among the clusters, there were some clear patterns in cluster groups in which the target was clearly yellowfin and some other patterns of mixed targets of yellowfin and bigeye tunas.

Conventional regression analysis

Full evaluation of models thought the model selection criterion has not yet reached, but comparison of results over the following models are shown in Figure 8. Also, the diagnostics and influence plots were shown in Figures 9 and 10.

Model 1: Quarterly LN: YrQ + LonLat

Model 2: Quarterly LN: YrQ + LonLat + Cluster

Model 3: Quarterly LN: YrQ + LonLat + Cluster + Vessel

*Model 4: Quarterly LN: YrQ + LonLat + Cluster + Vessel + Q*LonLat*

Model 5: Quarterly DL: Delta[YrQ + LonLat + Cluster] & Poisitve-LN[YrQ + LonLat + Cluster]

Model 6: Quarterly DL: Delta[YrQ + LonLat + Cluster] & Poisitve-LN[YrQ + LonLat + Cluster+Vessel]

- Decreasing patterns were similar over the different models in each region.
- In Region 4, there are lots of 0 data, and therefore the residuals plots for the LN model look ill-shaped. However, these unwanted shapes were improved enough when the DL model is applied.
- Computation for Model 6 in Region 4 was not achieved well perhaps because of a large number of 0 data. This might be resolved by analysing the data with selected clusters in which the yellowfin proportion is reasonably high.

WAYS FORWARD

Update of analysis using data up to 2020 fisheries

Because of the delay and difficulty in the data-sharingprocess, the results shown in this paper were still preliminary. Once 2020 data set is ready for use for re-clustering and re-standardization of CPUE, we will conduct our full analysis to provide a final set of results including VAST analysis based on the updated data

including 2020 fishery outcomes before the upcoming yellowfin stock assessment meeting scheduled in October 2021 for use as inputs for the update of its stock assessment. In addition, analyses can be further updated if some extra data are available from other longline countries. *(Note that there may not be enough data of size in 2020 due to COVID-19 pandemic)*

Evaluation of uncertainty

Although we have prepared "bootstrap option" for assessing the standard error and used it as a trial in each country's data, it takes long time to complete for the joint CPUE and therefore it was not used for the joint analysis yet. We will also report on this issue in case there is a significant difference or not.

Regional scaling factor

As future works, regional scaling will be applied for the conventional regression models so that a constant catchability can be assumed across the regions in the stock assessment models. The regional trends in the standardized CPUE are then compared to those from the VAST analysis, where catchability is constant by default and the regional scaling is not required.

Plan of submission

A final set of results based on the updated data including 2020 fishery outcomes will be submitted before the upcoming yellowfin stock assessment meeting scheduled in October 2021 for use as inputs for the update of its stock assessment.

REFERENCES

Amruthnath, N. and Gupta, T. 2019. Fault Diagnosis using Clustering. What Statistical Test to use for Hypothesis Testing? Machine Learning and Applications. doi:10.5121/mlaij.2019.6102

Bentley, N., Kendrick, T.H., Starr. P.J. and Breen P.A. 2012. Influence plots and metrics: tools for better understanding fisheries catch-per-unit-effort standardizations. ICES J. Mar. Sci. 69(1): 84-88.

He, X., Bigelow, K.A., Boggs, C.H. 1997. Cluster analysis of longline sets and fishing strategies within the Hawaii-based fishery. Fish. Res. 31: 147-158.

Hoyle, S.D., Chang, S.T., Fu. D., Kim, D.N., Lee, S.I., Matsumoto, T., Chassot, E. and Yeh, Y.M. (2019a) Collaborative study of bigeye and yellowfin tuna CPUE from multiple Indian Ocean longline fleets in 2019, with consideration of discarding. IOTC-2019-WPM10-16.

Hoyle, S.D., Chassot, E., Fu, D., Kim, D.N., Lee, S.I., Matsumoto, T., Satoh, K., Wang, S.P. and Kitakado, T. (2019b) Collaborative study of albacore tuna CPUE from multiple Indian Ocean longline fleets in 2019. IOTC-2019-WPTmT07(DP)-19.

Hoyle, S.D., Kitakado, T., Yeh, Y.M., Wang, S.P., Wu, R.F., Chang, F.C., Matsumoto, T., Satoh, K., Kim, D.N., Lee, S.I., Chassot, E., and Fu, D. (2018) Report of the Fifth IOTC CPUE Workshop on Longline Fisheries, May 28th–June 1st, 2018. IOTC–2018–CPUEWS05–R. 27 pp.

Hoyle, S.D., Langley, A.D. 2020 Scaling factors for multi-region stock assessments, with an application to Indian Ocean tropical tuans. Fish. Res. 228 https://doi.org/10.1016/j.fishres.2020.105586

Kitakado, T., Satoh, K., Matsumoto, T., Yokoi, H., Okamoto, K., Lee, S., Lee, M., Lim, J., Wang, S., Su, N., Tsai, W., Chang, S. and Kitakado, T. 2020. Plan of trilateral collaborative study among Japan, Korea and Taiwan for producing joint abundance index with longline fisheries data for the tropical tuna species in the Indian Ocean. Collect. IOTC-2020-WPTT22(SA)-09.

Lee, S.I, Lim J.H., Lee, M.K. and Kwon, Y., 2021 CPUE standardization of yellowfin tuna caught by Korean tuna longline fishery in the Indian Ocean, 1979-2019. IOTC-2021-WPTT(DP)-INF03.

Matsumoto, T. 2021 Review of Japanese fisheries and tropical tuna catch in the Indian Ocean. IOTC-2021-WPTT23(DP)-INF01.

Matsumoto, T., Satoh, K. and Yokoi, H. 2021. Japanese longline CPUE for yellowfin tuna in the Indian Ocean standardized by generalized linear model which includes cluster analysis. IOTC-2021-WPTT(DP)-INF02.

Thorson, J.T., Barnett, L.A.K., 2017. Comparing estimates of abundance trends and distribution shifts using single- and multispecies models of fishes and biogenic habitat. ICES J. Mar. Sci. 74, 1311–1321.

Thorson, J.T., 2019. Guidance for decisions using the Vector Autoregressive Spatio-Temporal (VAST) package in stock, ecosystem, habitat and climate assessments. Fish. Res. 210, 143–161.

(a) Japan

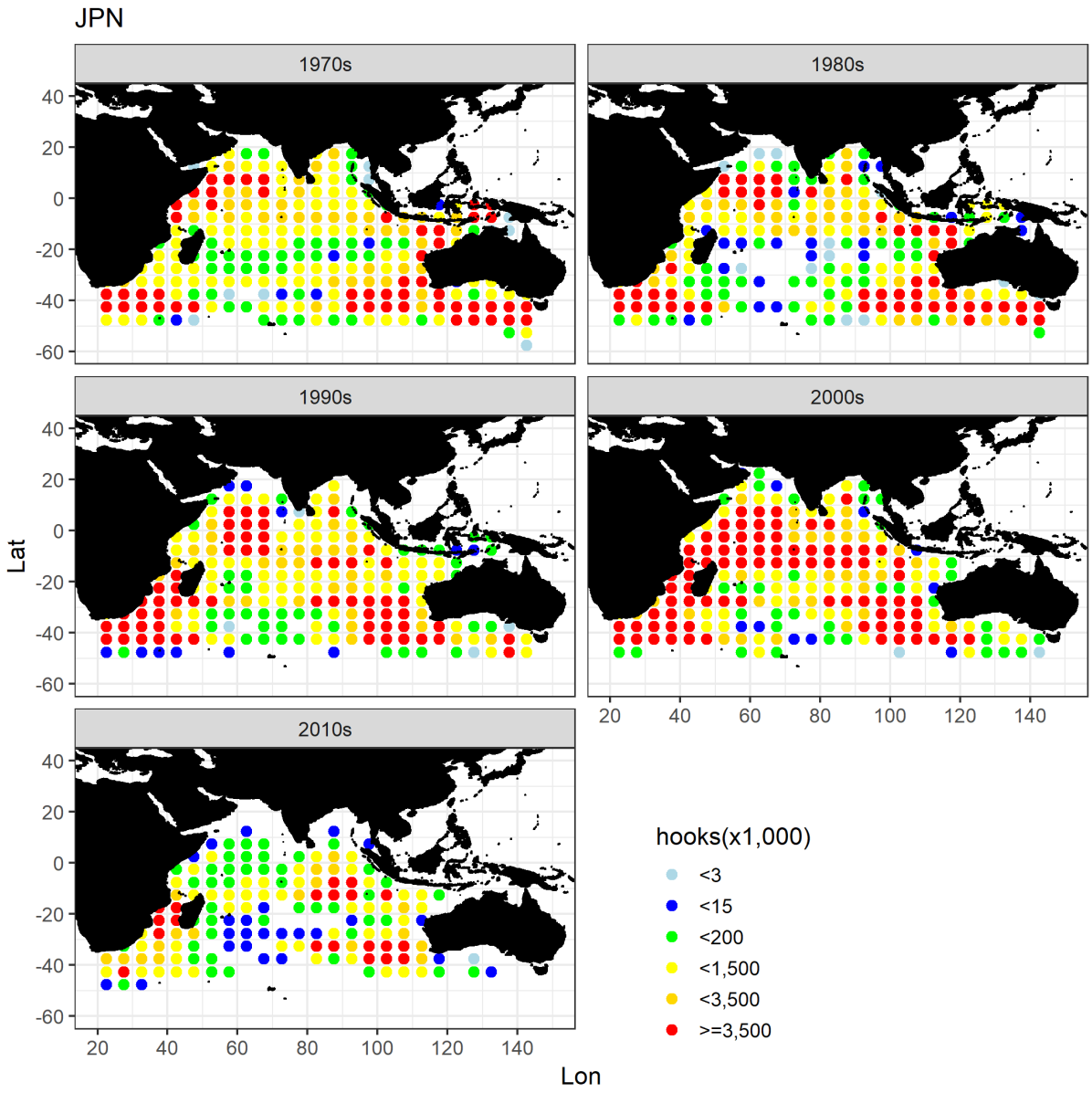

Figure 1: Decadal distributions of fishing efforts (number of hooks) for longline fisheries over the fishing ground in the IOTC convention area. (extracted from Matsumoto, 2021)

(b) Korea

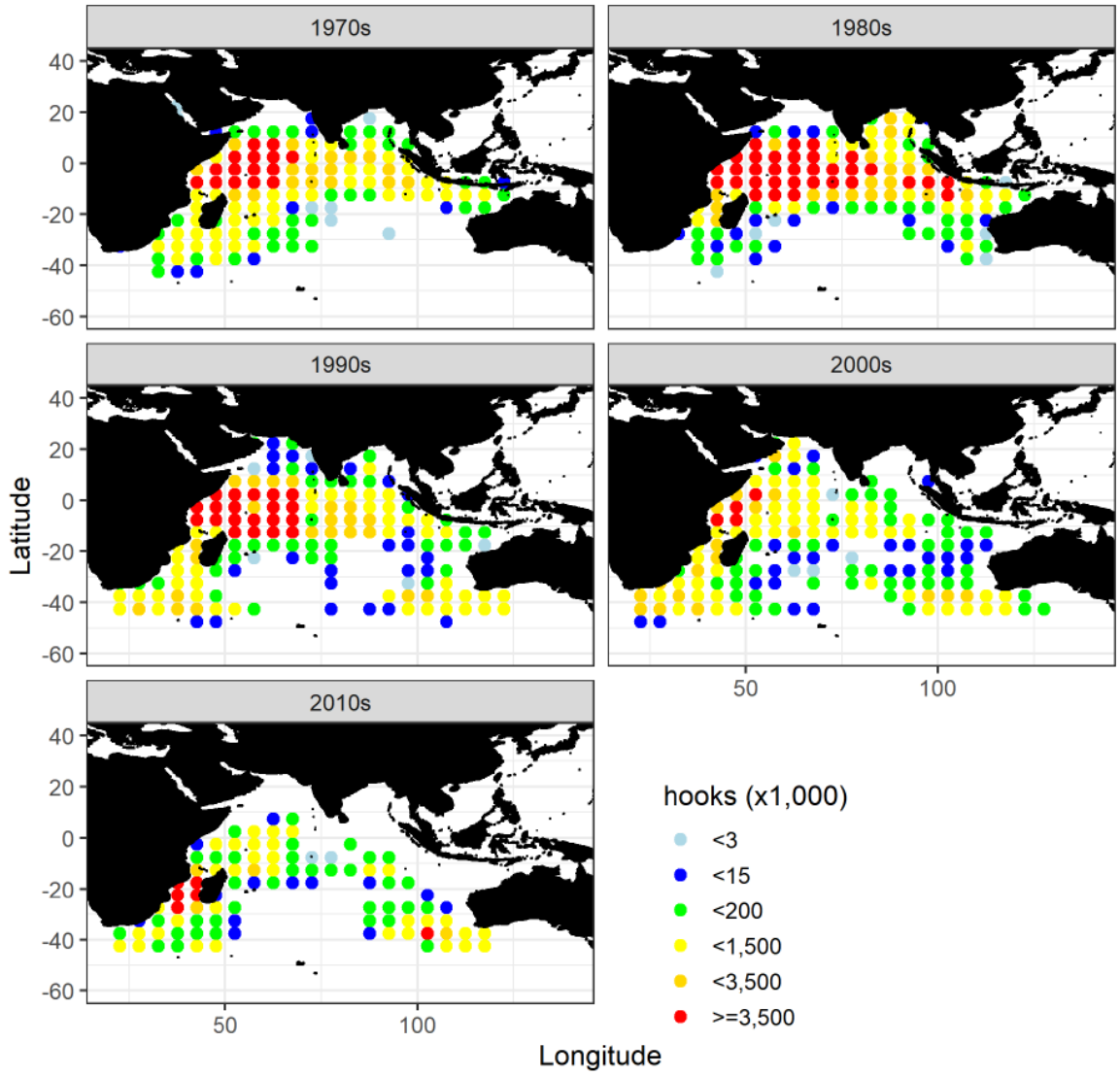

Figure 1 (Continued) : For Korean fishery (extracted from Lee et al., 2021).

(c) Taiwan

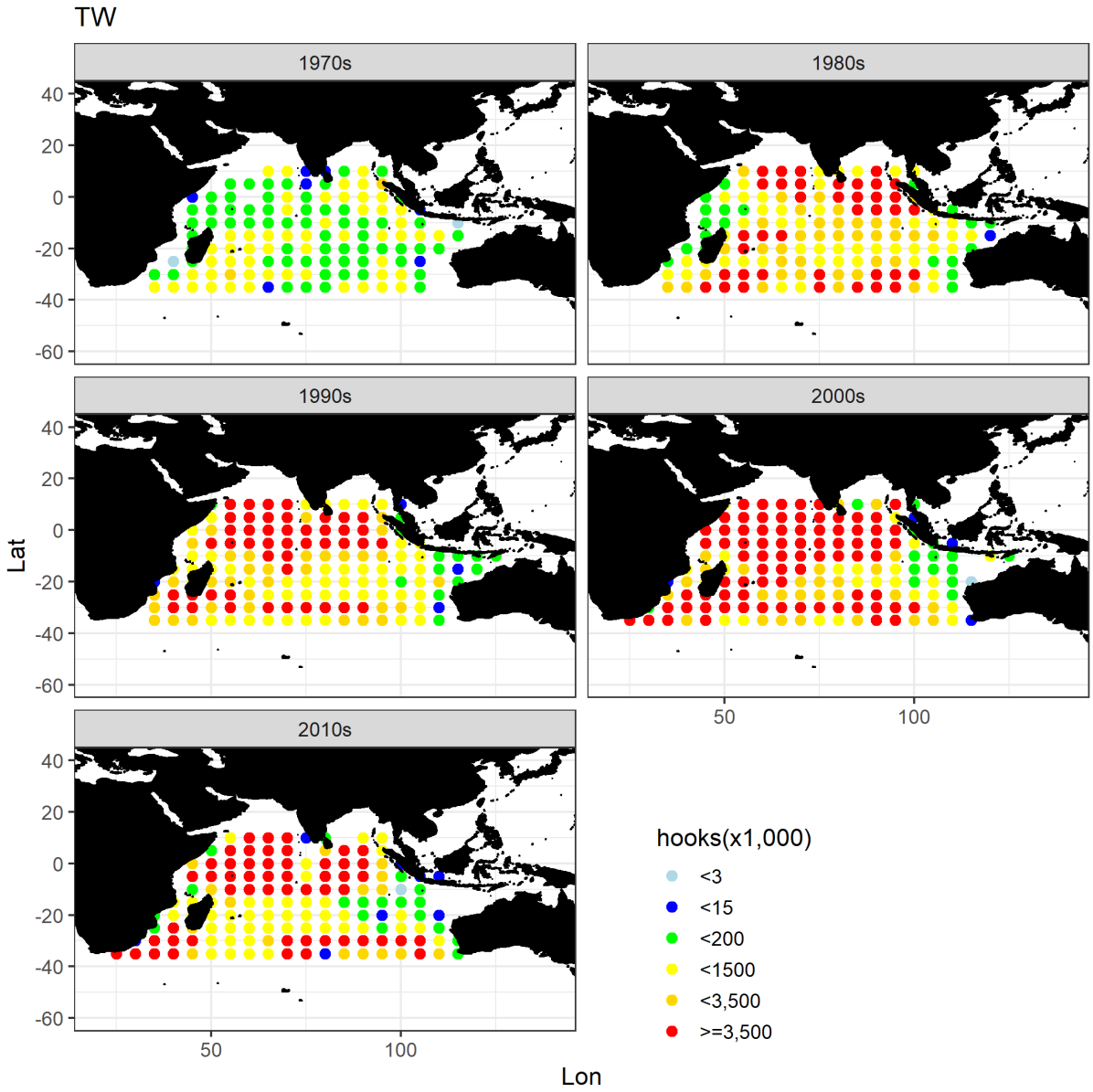

Figure 1 (Continued): For Taiwanese fishery.

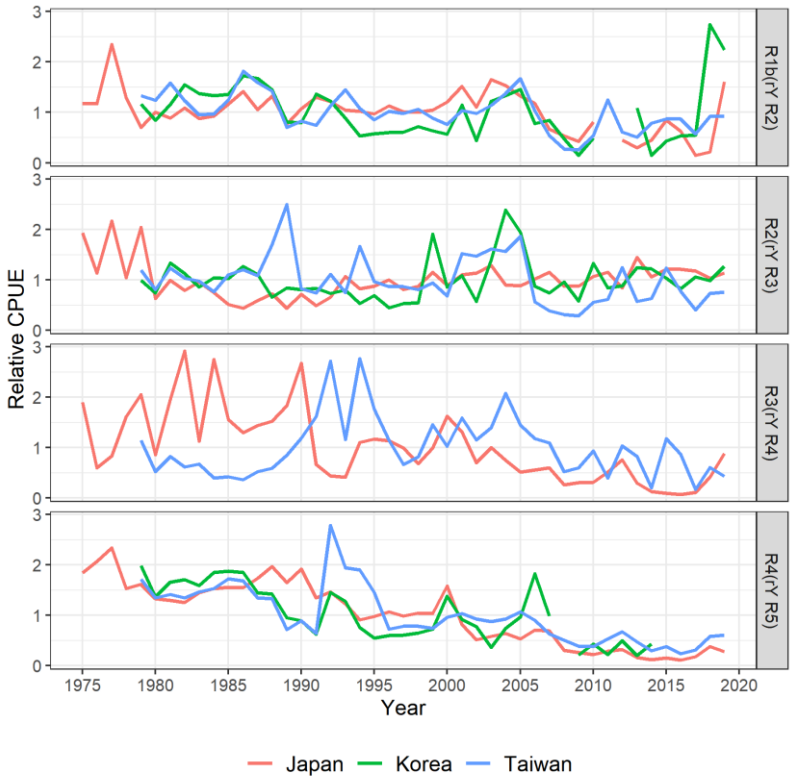

Figure 2: Time series of the nominal CPUE for yellowfin tuna by the longline fisheries in the IOTC convention area.

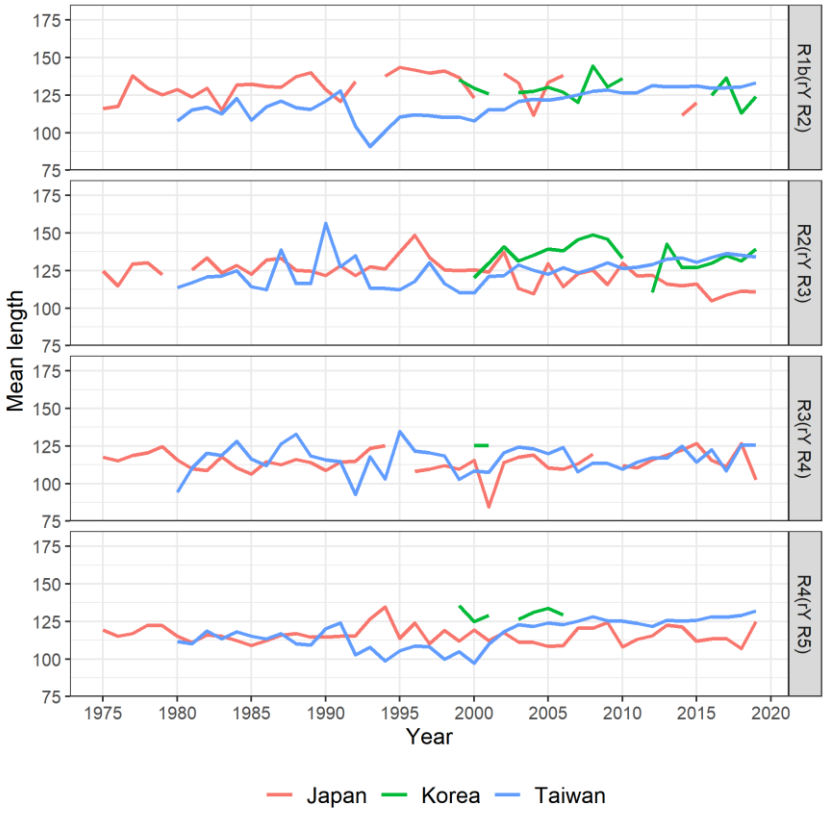

Figure 3: Time series of the mean length of yellowfin tuna caught by the longline fisheries in the IOTC convention area.

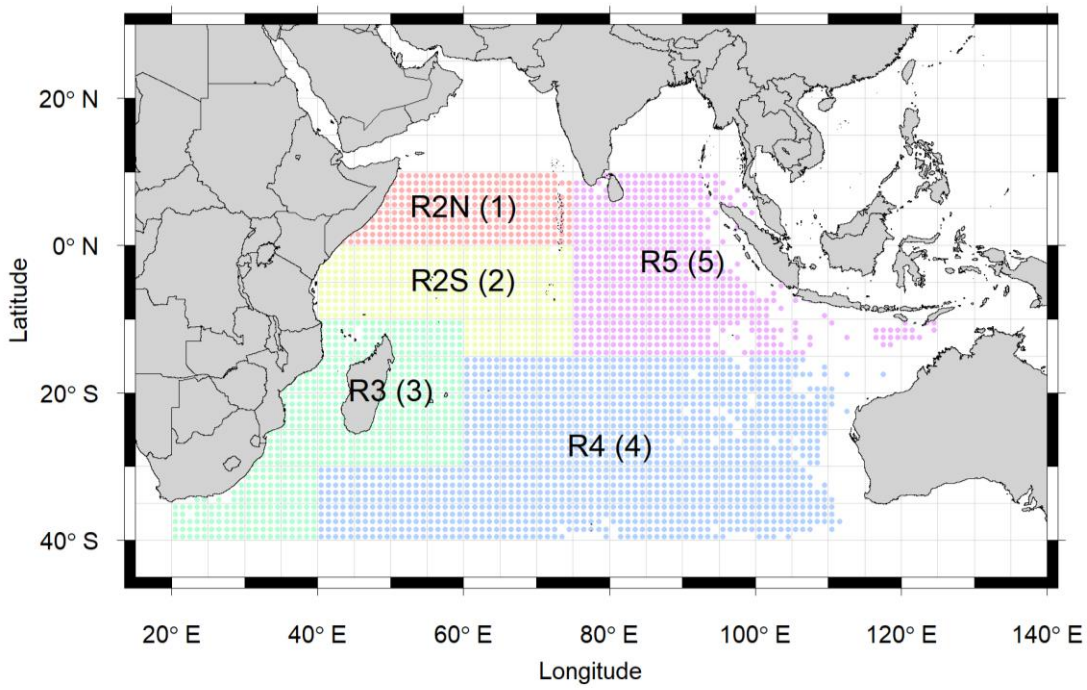

Figure 4: Map of the regional structures used in the joint CPUE indices for yellowfin tunas.

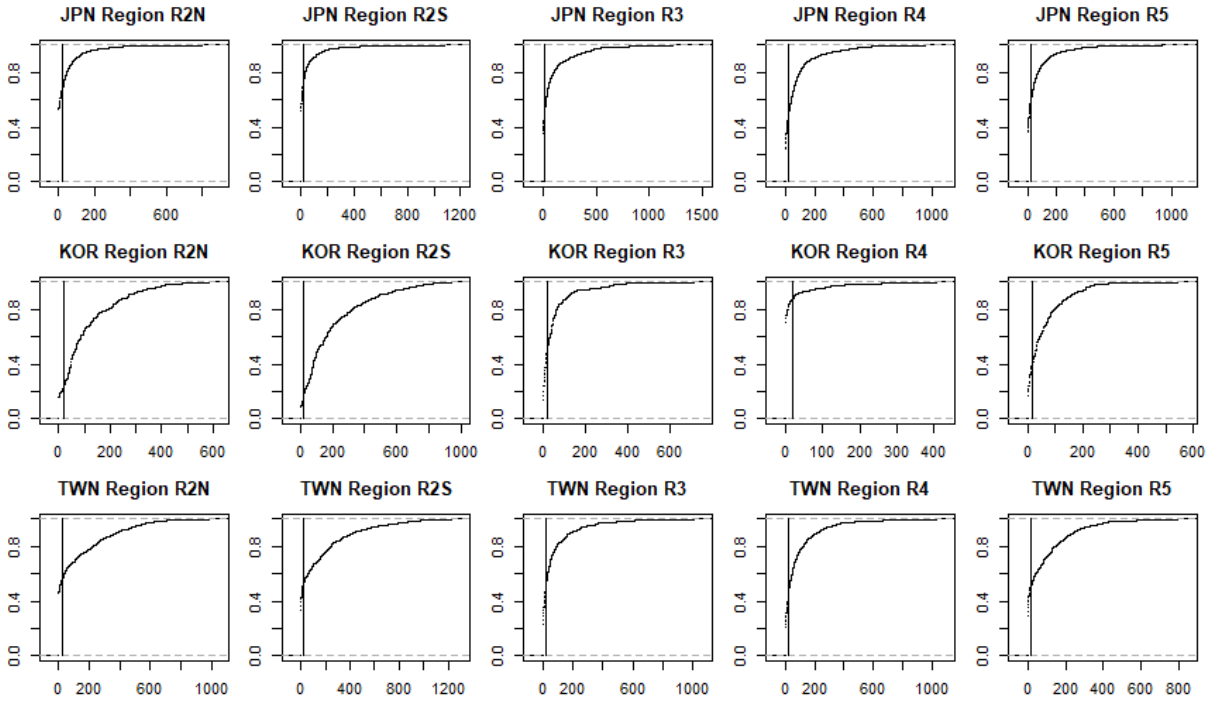

Figure 5: Empirical distribution of the vessel-wise number of data set in each Region in each country. The vertical line is at a threshold value of 20.

(Original data)

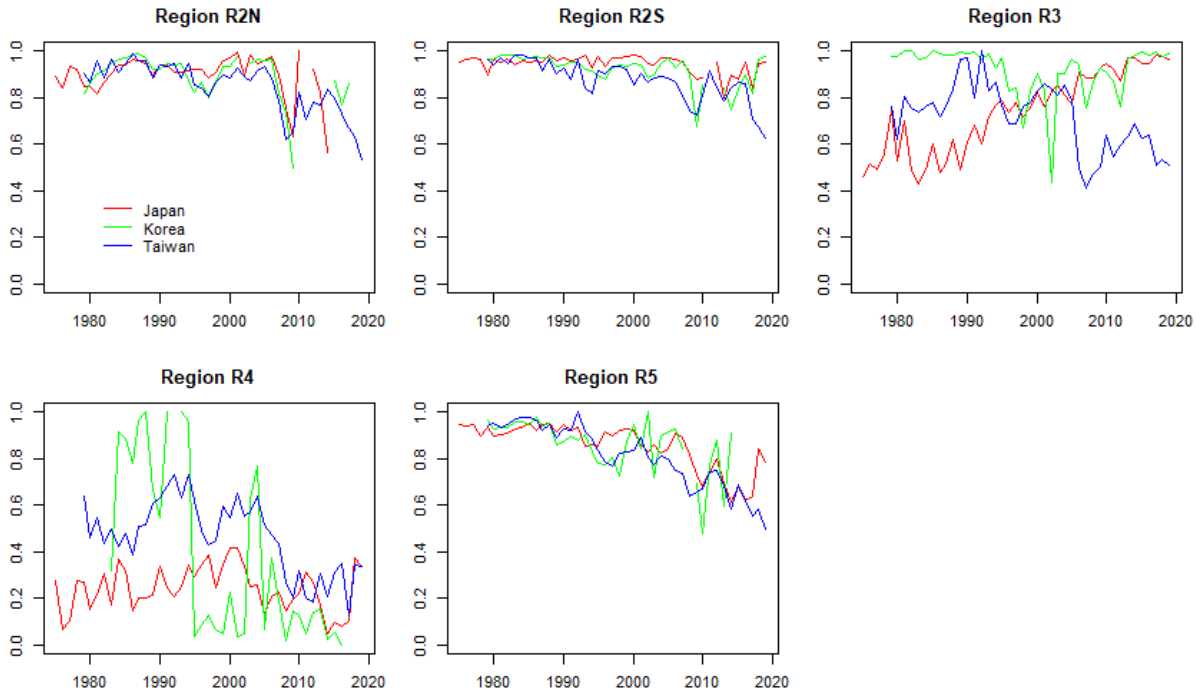

(Screened data)

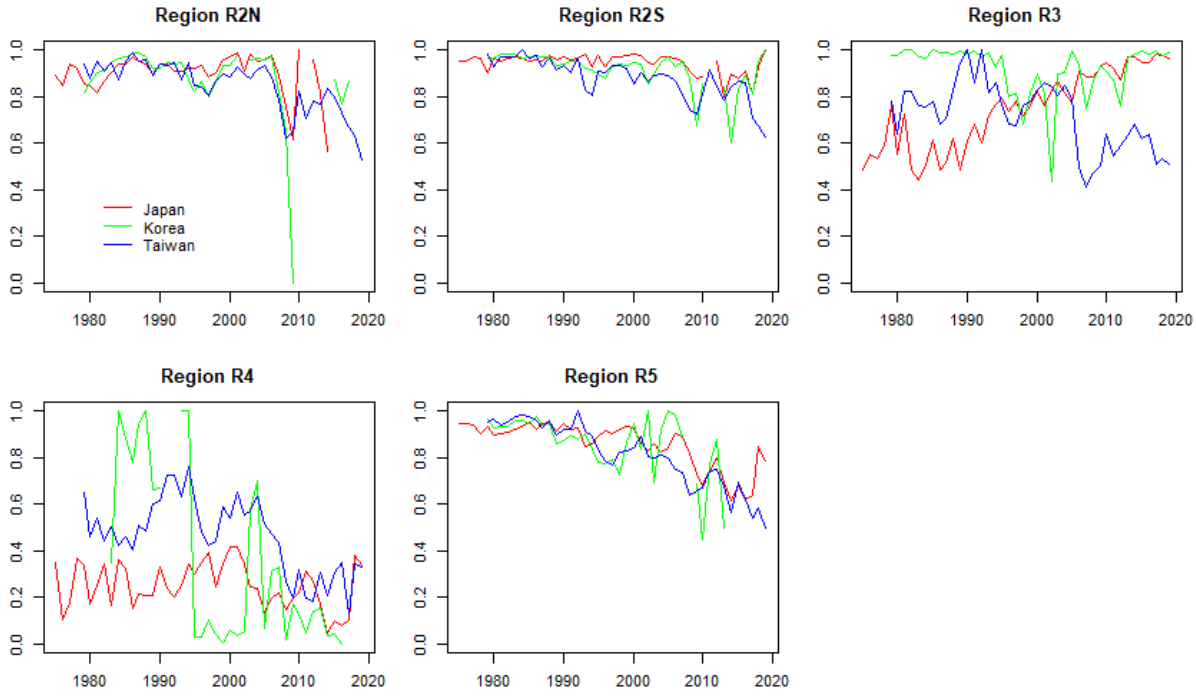

Figure 6: Time series of positive probability rates in different regions before applying the threshold value of the number of operations.

(a) Japan

R2

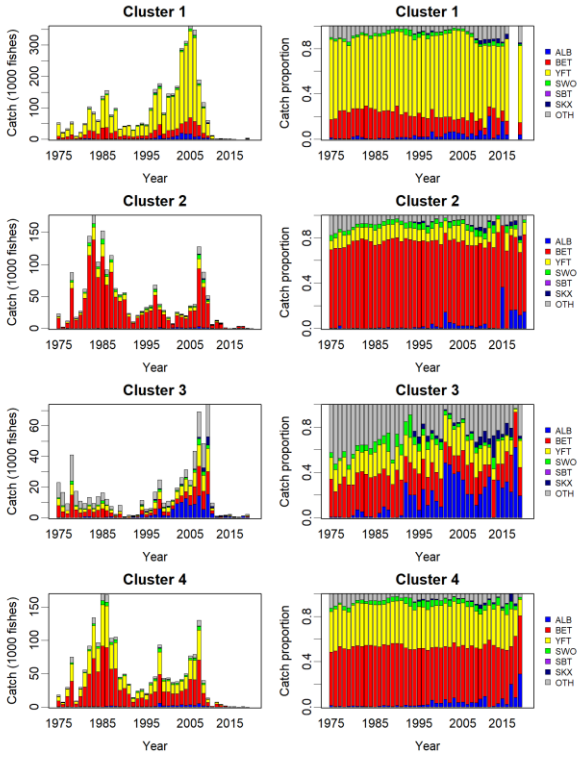

R3

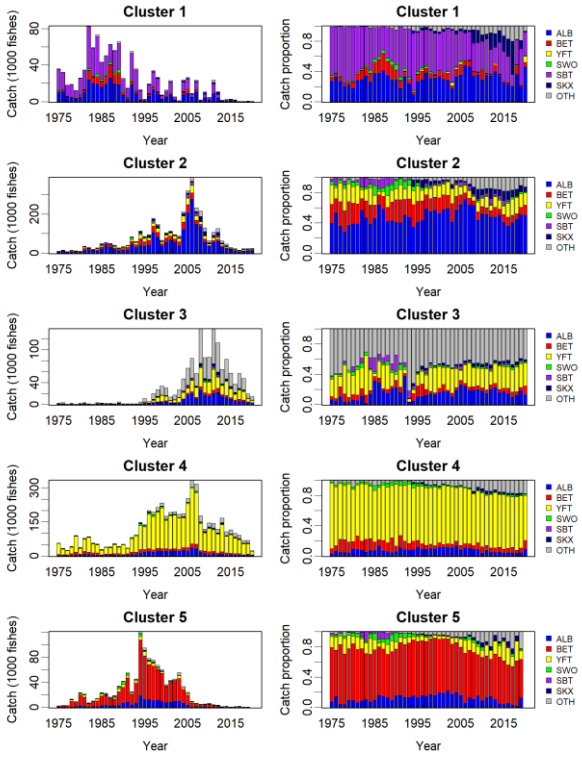

R4

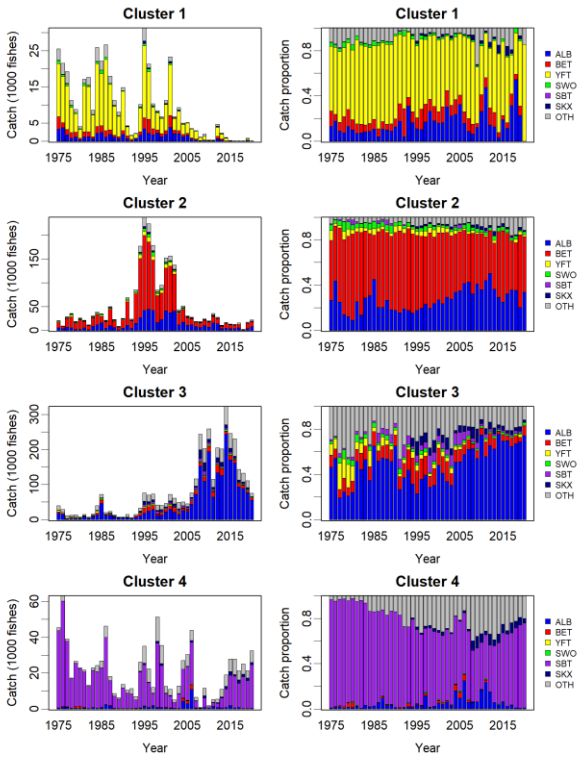

R5

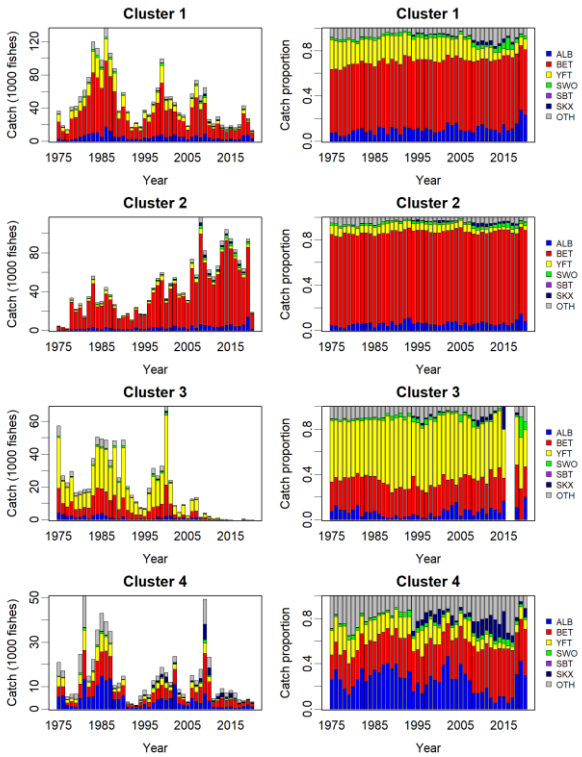

Figure 7(a): Species composition for each cluster in Japanese fisheries (extracted from Matsumoto et al. 2021).

(b) Korea

R2

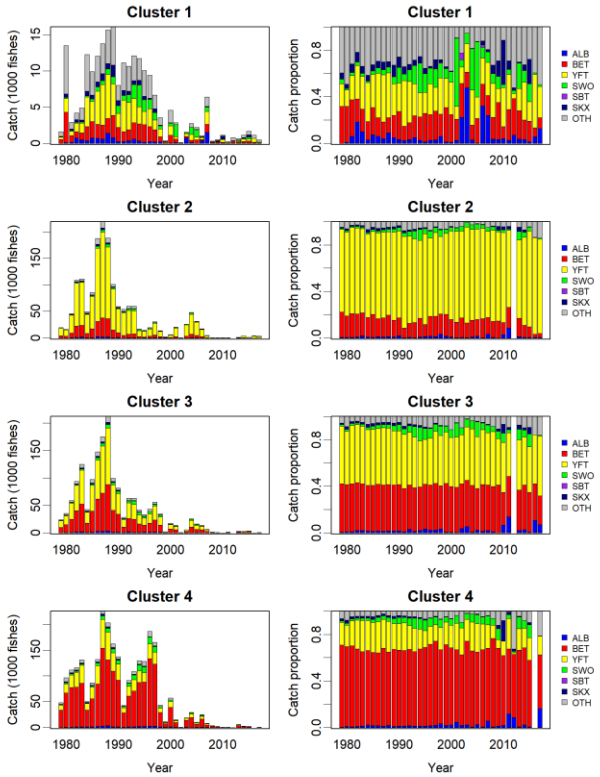

R3

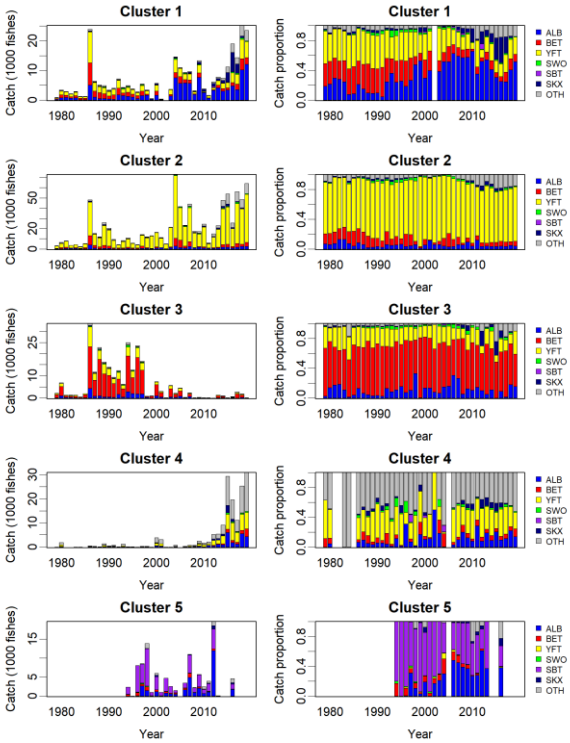

R4

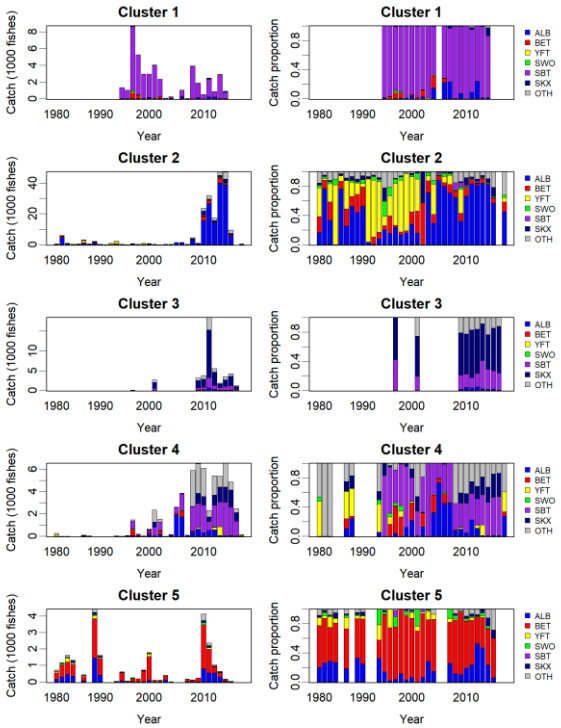

R5

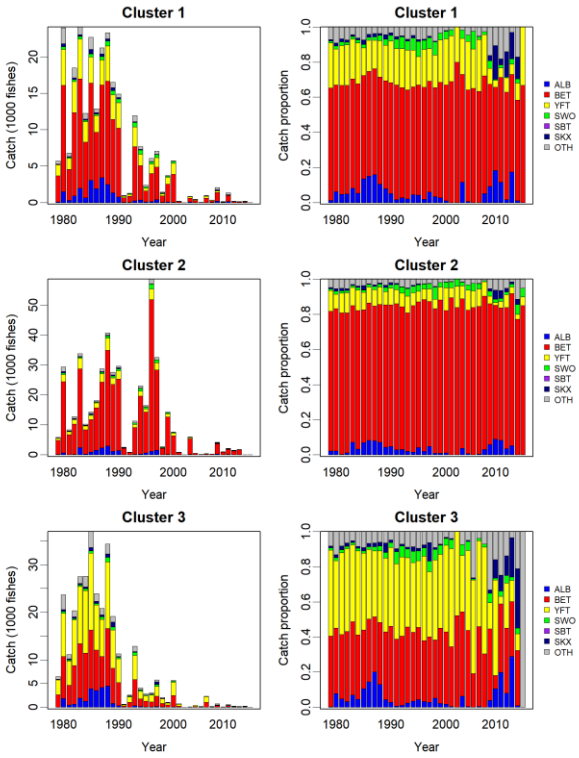

Figure 7(b): Species composition for each cluster in Korean fisheries (extracted from Lee et al. 2021).

(c) Taiwan

R2

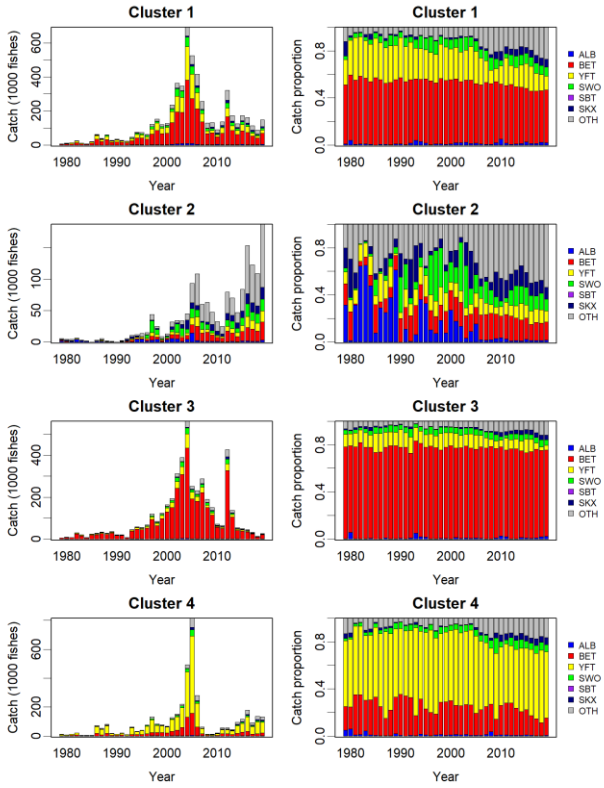

R3

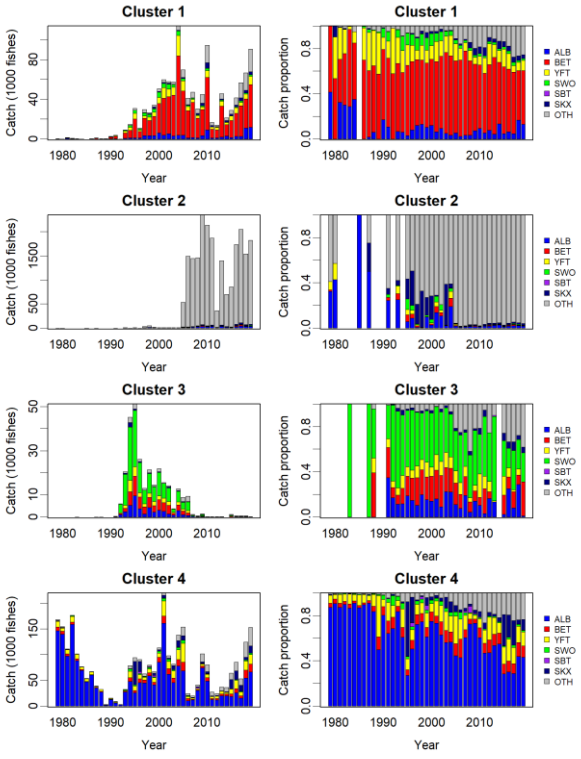

R4

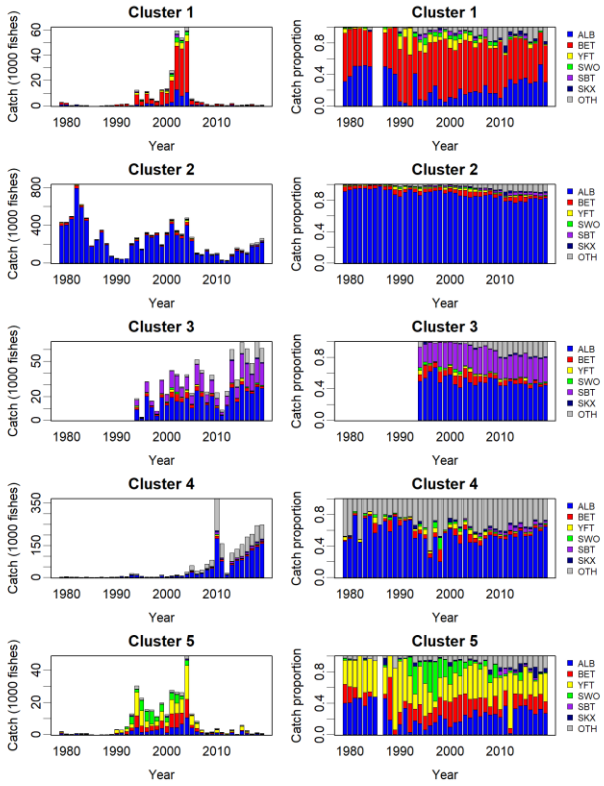

R5

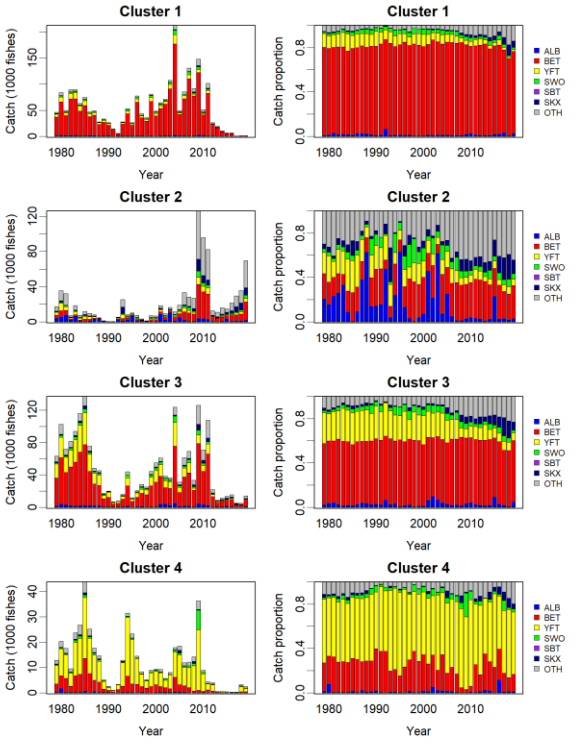

Figure 7(c): Species composition for each cluster in Taiwanese fisheries.

(~ YrQ + LonLat)

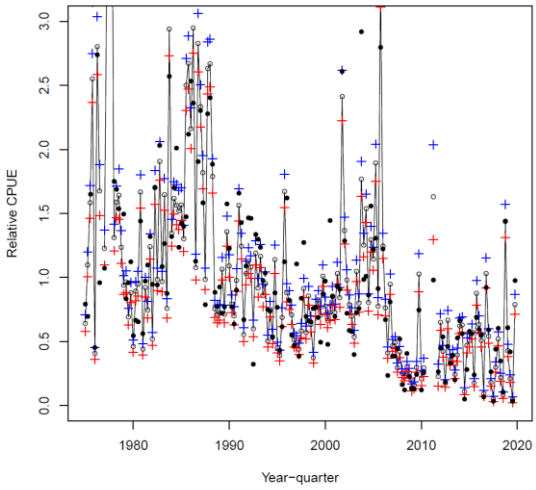

(~ YrQ + LonLat + Cluster)

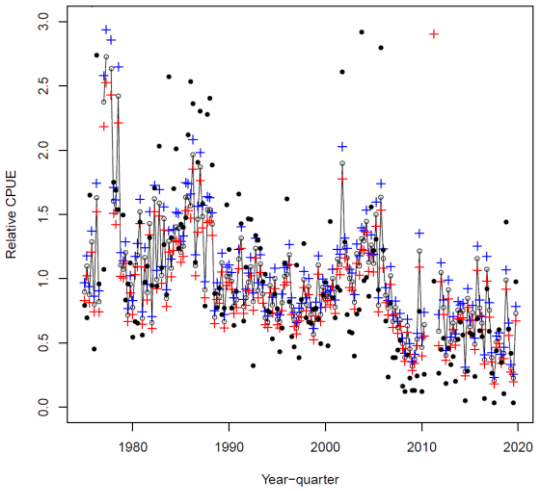

(~ YrQ + LonLat + Cluster + Vessel)

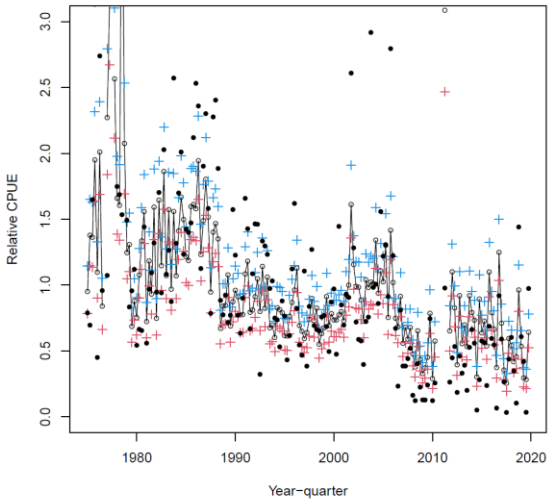

(~ YrQ+LonLat+Cluster+Vessel+Q*LonLat)

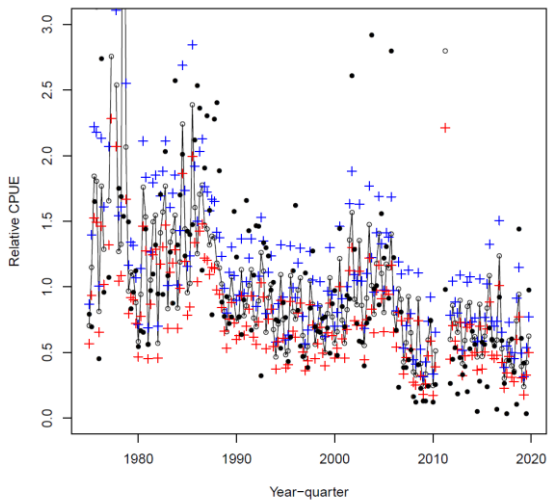

D[YrQ + LonLat + Cluster] & LN[YrQ + LonLat + Cluster]

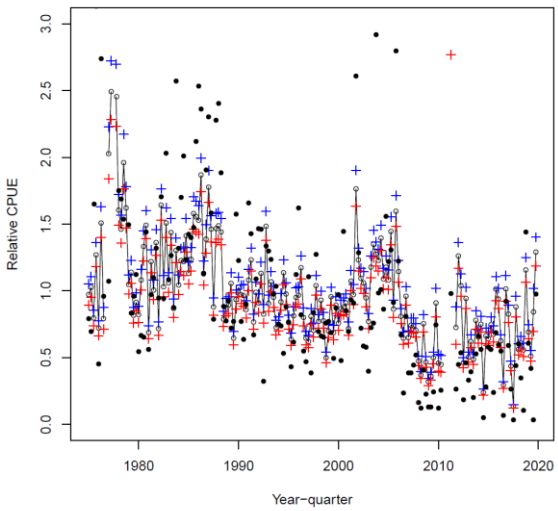

D[YrQ + LonLat + Cluster] & LN[YrQ + LonLat + Cluster+Vessel]

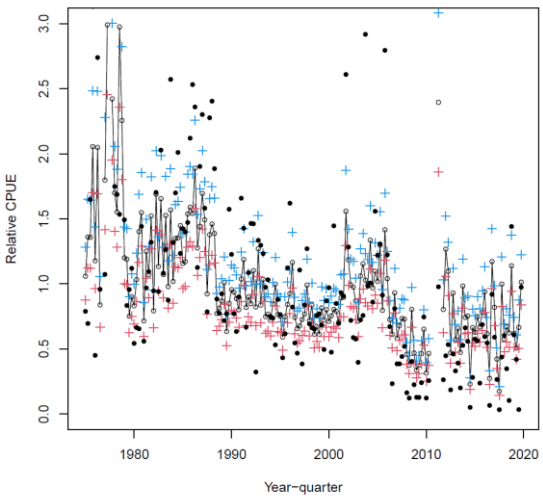

Figure 8(a): Nominal (black circles) and estimated annual indices (line with open circles) with 95% CI in R2N.

(~ YrQ + LonLat)

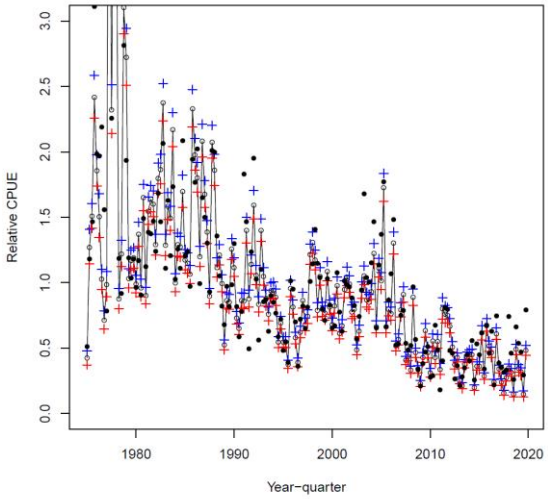

(~ YrQ + LonLat + Cluster)

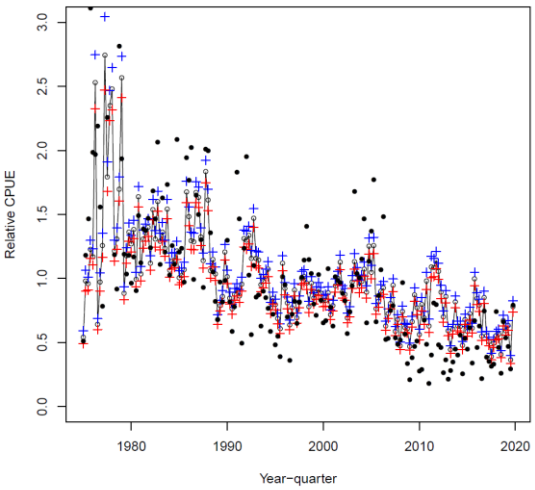

(~ YrQ + LonLat + Cluster + Vessel)

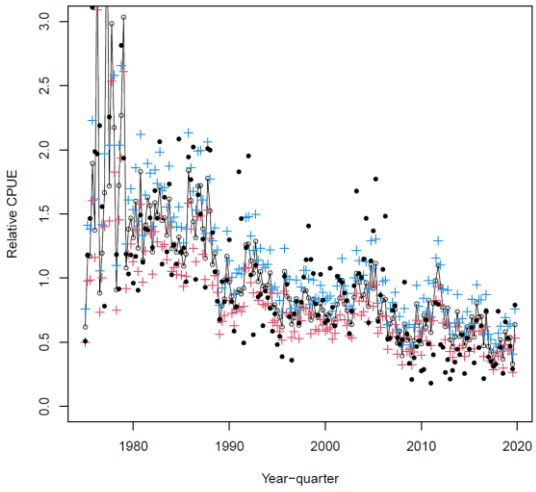

(~ YrQ+LonLat+Cluster+Vessel+Q*LonLat)

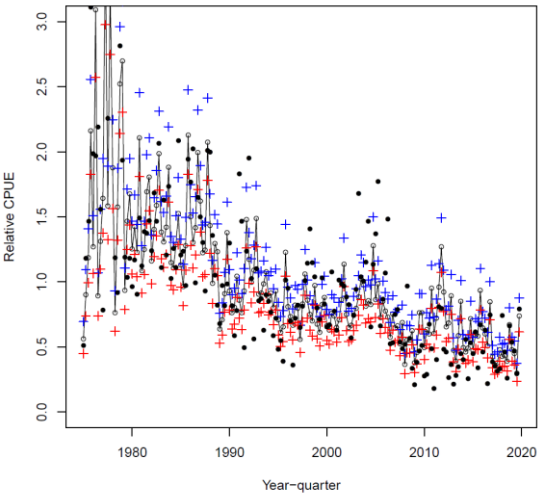

D[YrQ + LonLat + Cluster] & LN[YrQ + LonLat + Cluster]

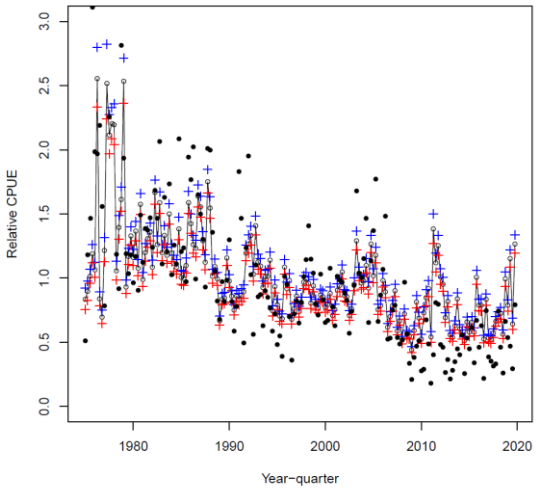

D[YrQ + LonLat + Cluster] & LN[YrQ + LonLat + Cluster+Vessel]

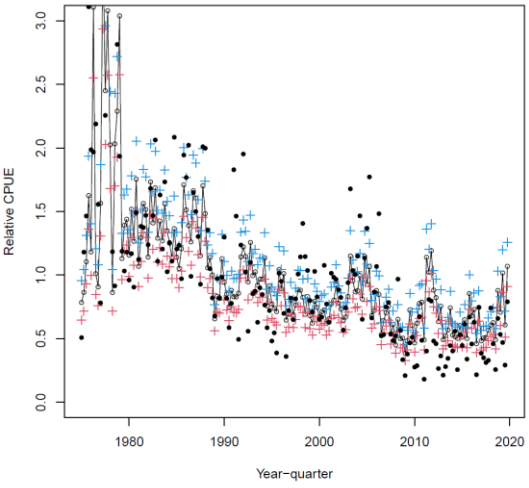

Figure 8(b): Nominal (black circles) and estimated annual indices (line with open circles) with 95% CI in R2S.

(~ YrQ + LonLat)

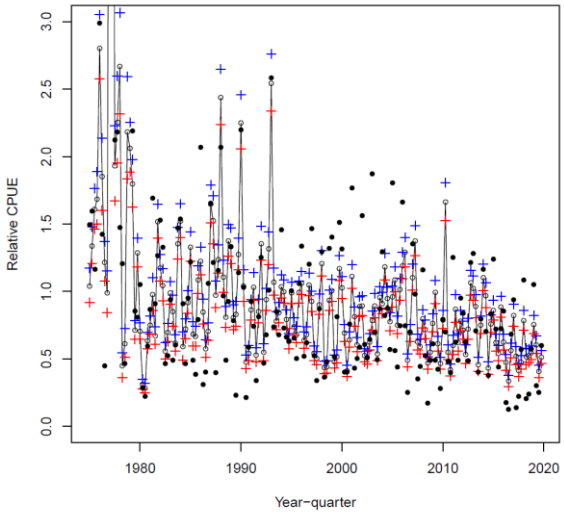

(~ YrQ + LonLat + Cluster)

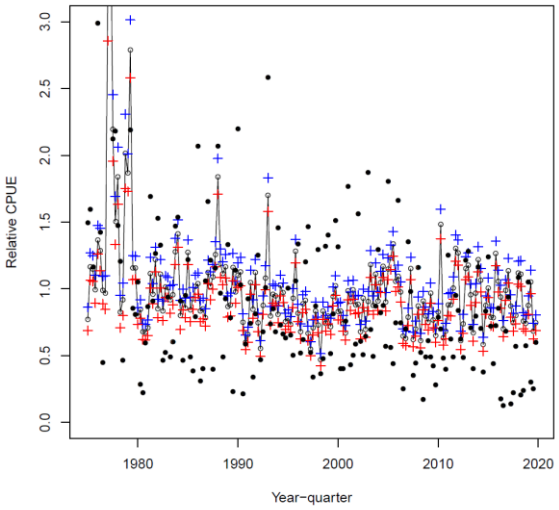

(~ YrQ + LonLat + Cluster + Vessel)

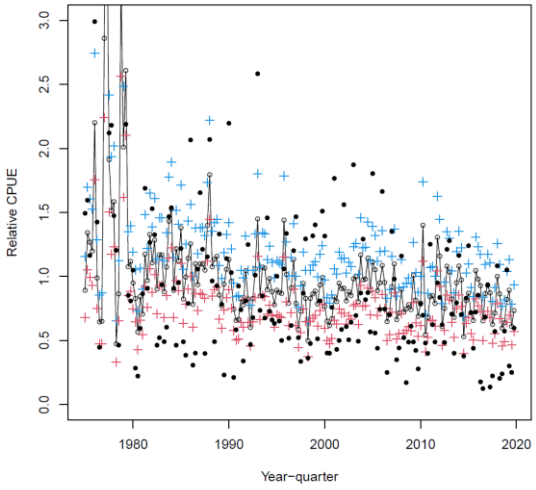

(~ YrQ+LonLat+Cluster+Vessel+Q*LonLat)

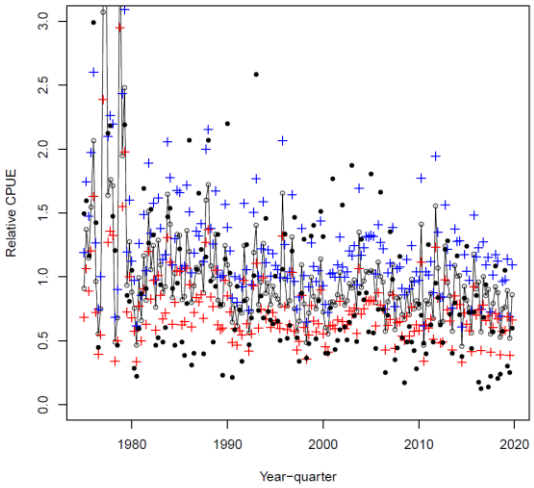

D[YrQ + LonLat + Cluster] & LN[YrQ + LonLat + Cluster]

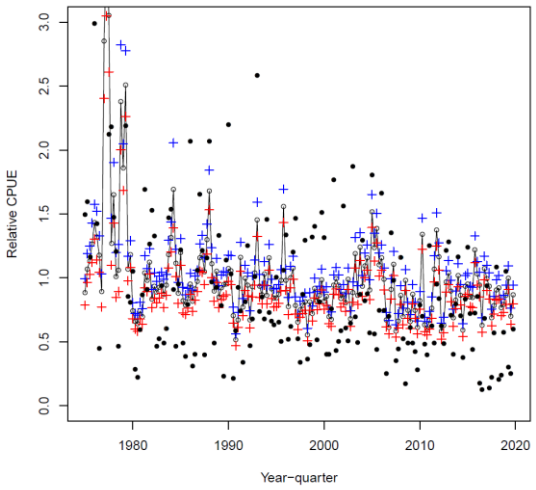

D[YrQ + LonLat + Cluster] & LN[YrQ + LonLat + Cluster+Vessel]

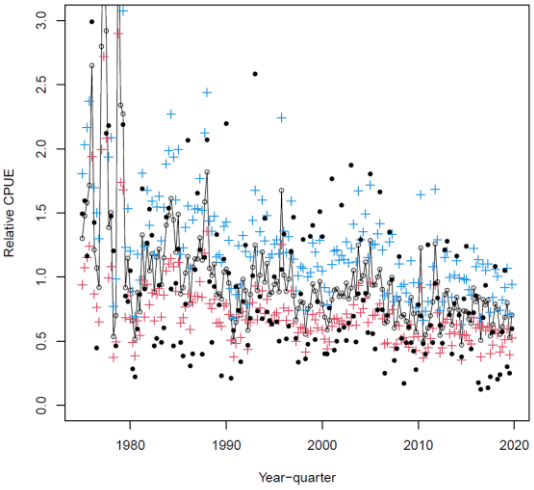

Figure 8(c): Nominal (black circles) and estimated annual indices (line with open circles) with 95% CI in R3.

(~ YrQ + LonLat)

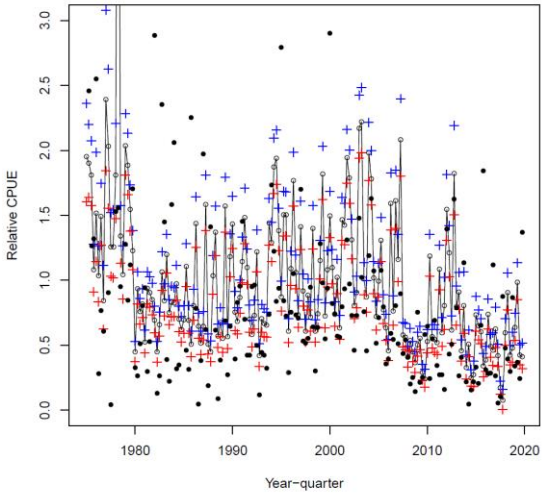

(~ YrQ + LonLat + Cluster)

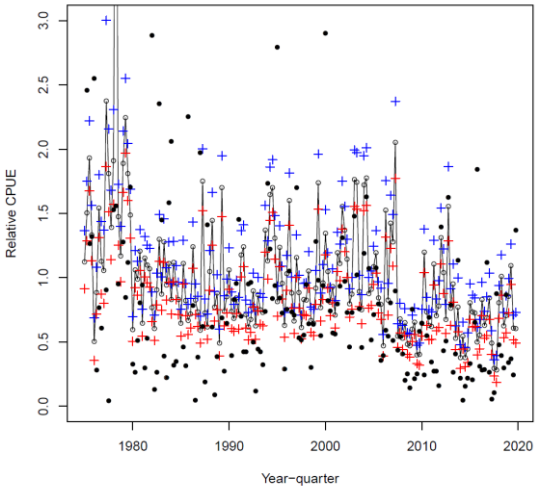

(~ YrQ + LonLat + Cluster + Vessel)

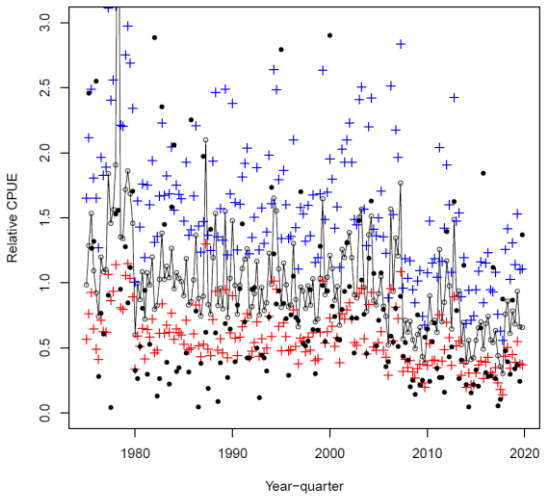

(~ YrQ+LonLat+Cluster+Vessel+Q*LonLat)

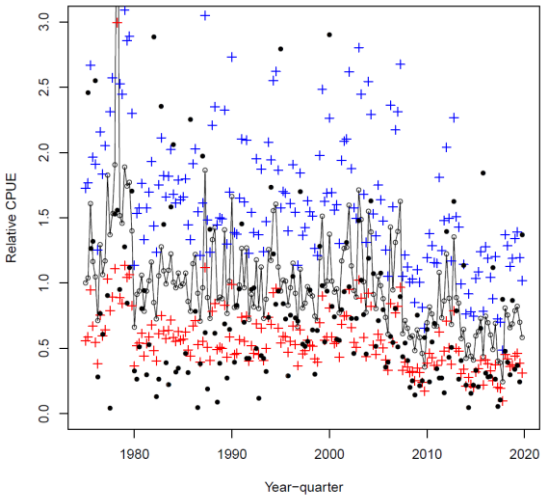

D[YrQ + LonLat + Cluster] & LN[YrQ + LonLat + Cluster]

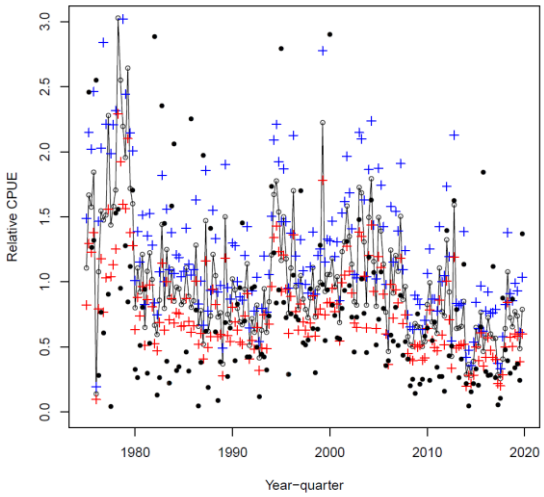

D[YrQ + LonLat + Cluster] & LN[YrQ + LonLat + Cluster+Vessel]

Figure 8(d): Nominal (black circles) and estimated annual indices (line with open circles) with 95% CI in R4.

(~ YrQ + LonLat)

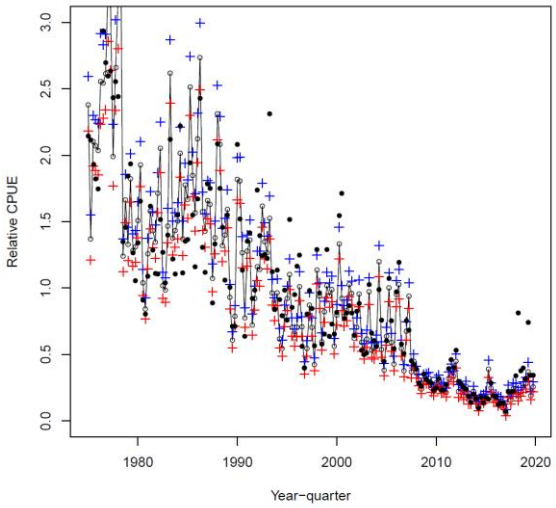

(~ YrQ + LonLat + Cluster)

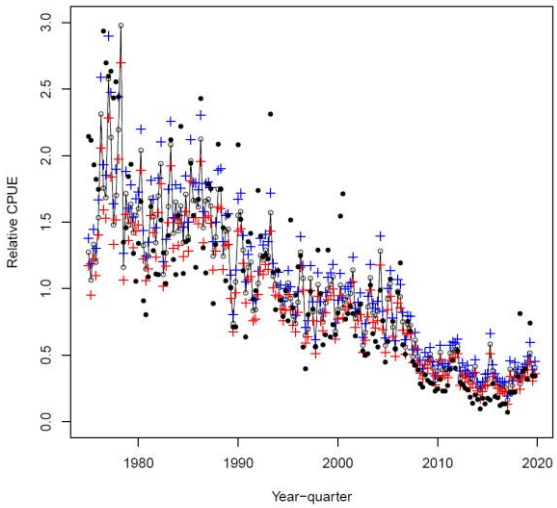

(~ YrQ + LonLat + Cluster + Vessel)

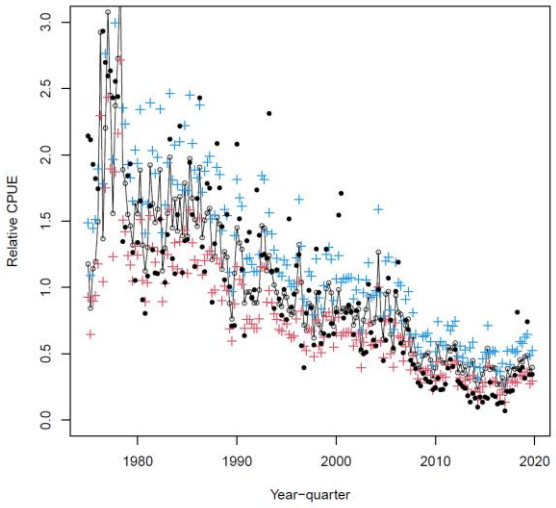

(~ YrQ+LonLat+Cluster+Vessel+Q*LonLat)

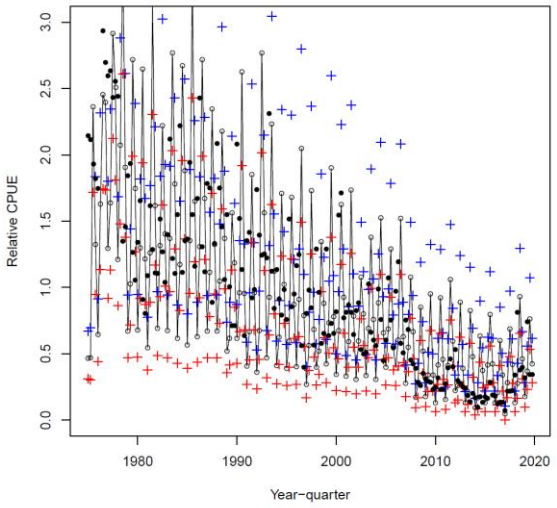

D[YrQ + LonLat + Cluster] & LN[YrQ + LonLat + Cluster]

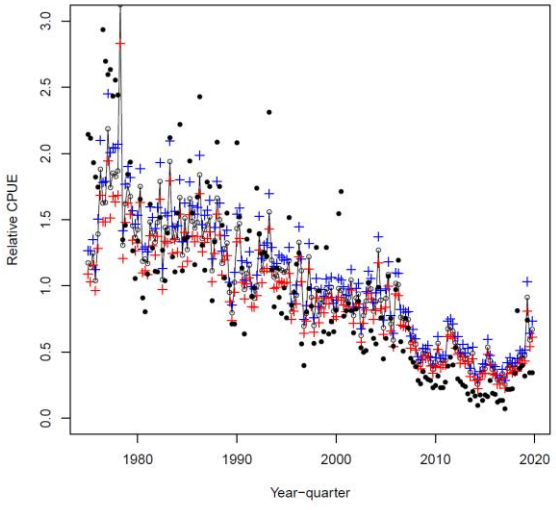

D[YrQ + LonLat + Cluster] & LN[YrQ + LonLat + Cluster+Vessel]

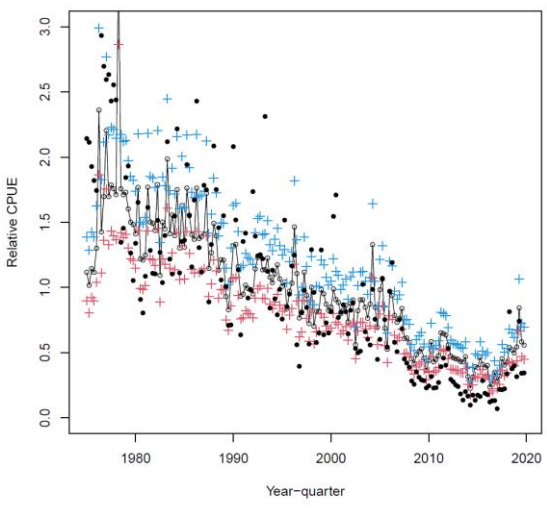

Figure 8(e): Nominal (black circles) and estimated annual indices (line with open circles) with 95% CI in R5.

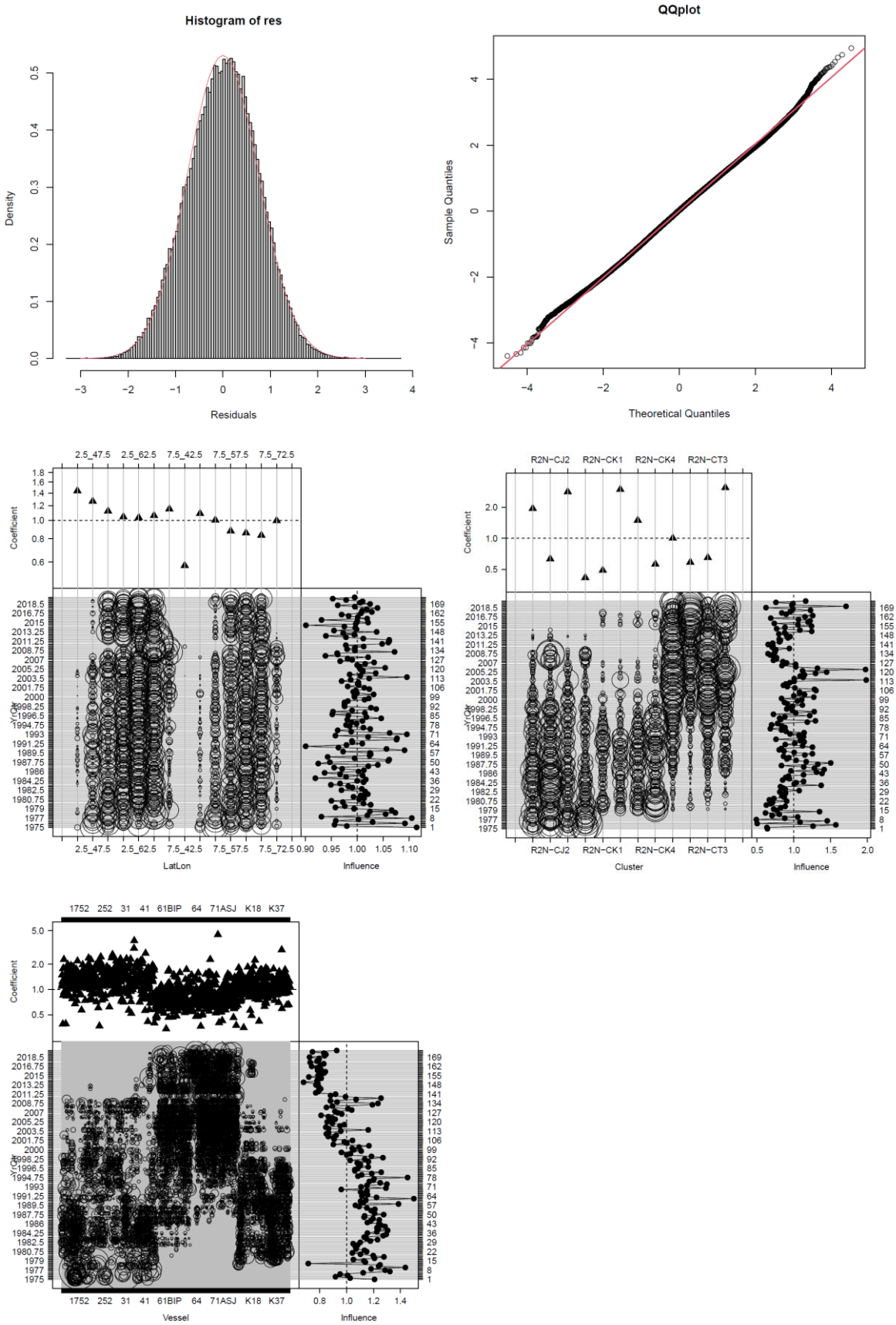

Figure 9(a): Diagnostics and influence plots for LN(~ YrQ + LonLat + Cluster+Vessel) for R2N.

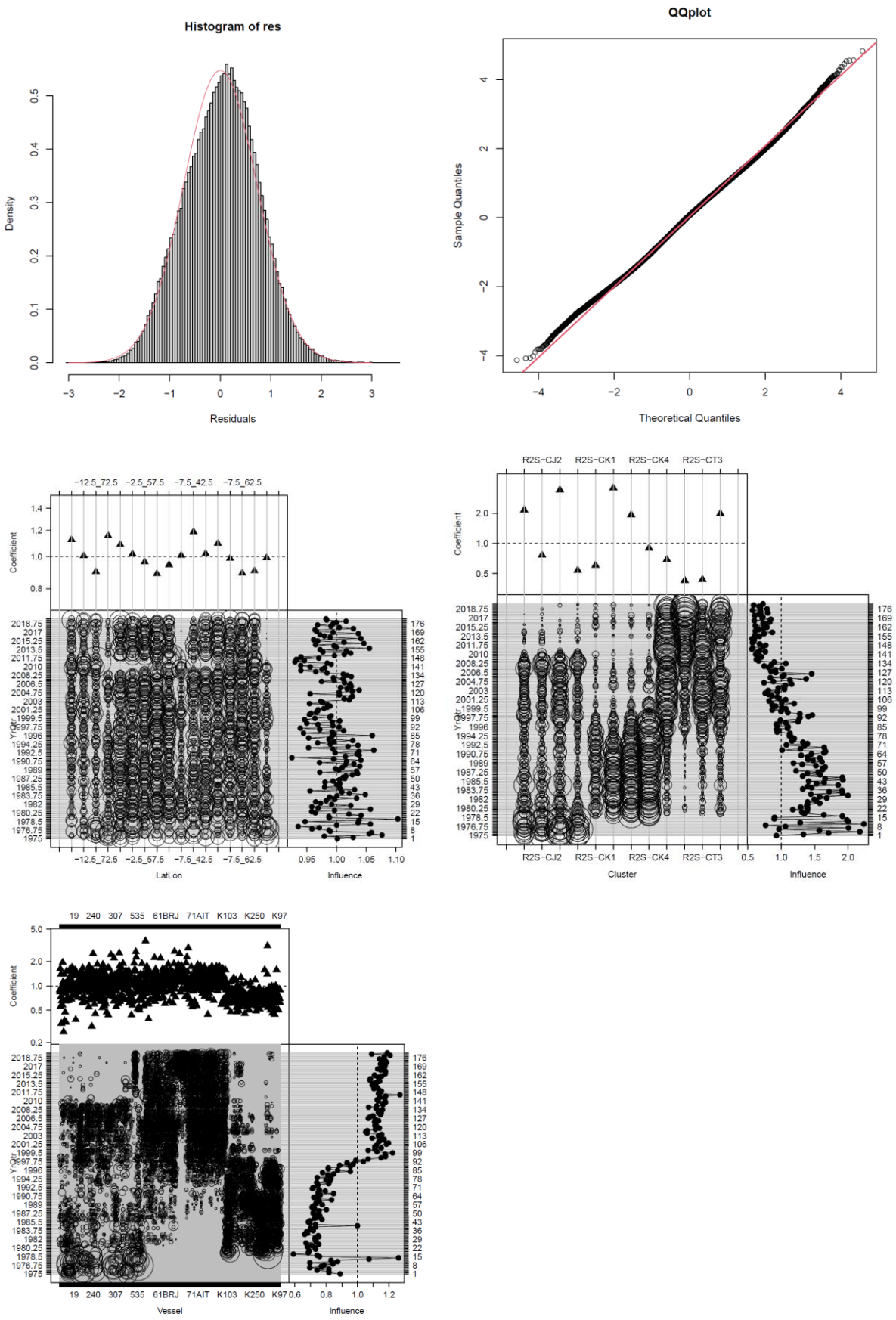

Figure 9(b): Diagnostics and influence plots for LN(~ YrQ + LonLat + Cluster+Vessel) for R2S.

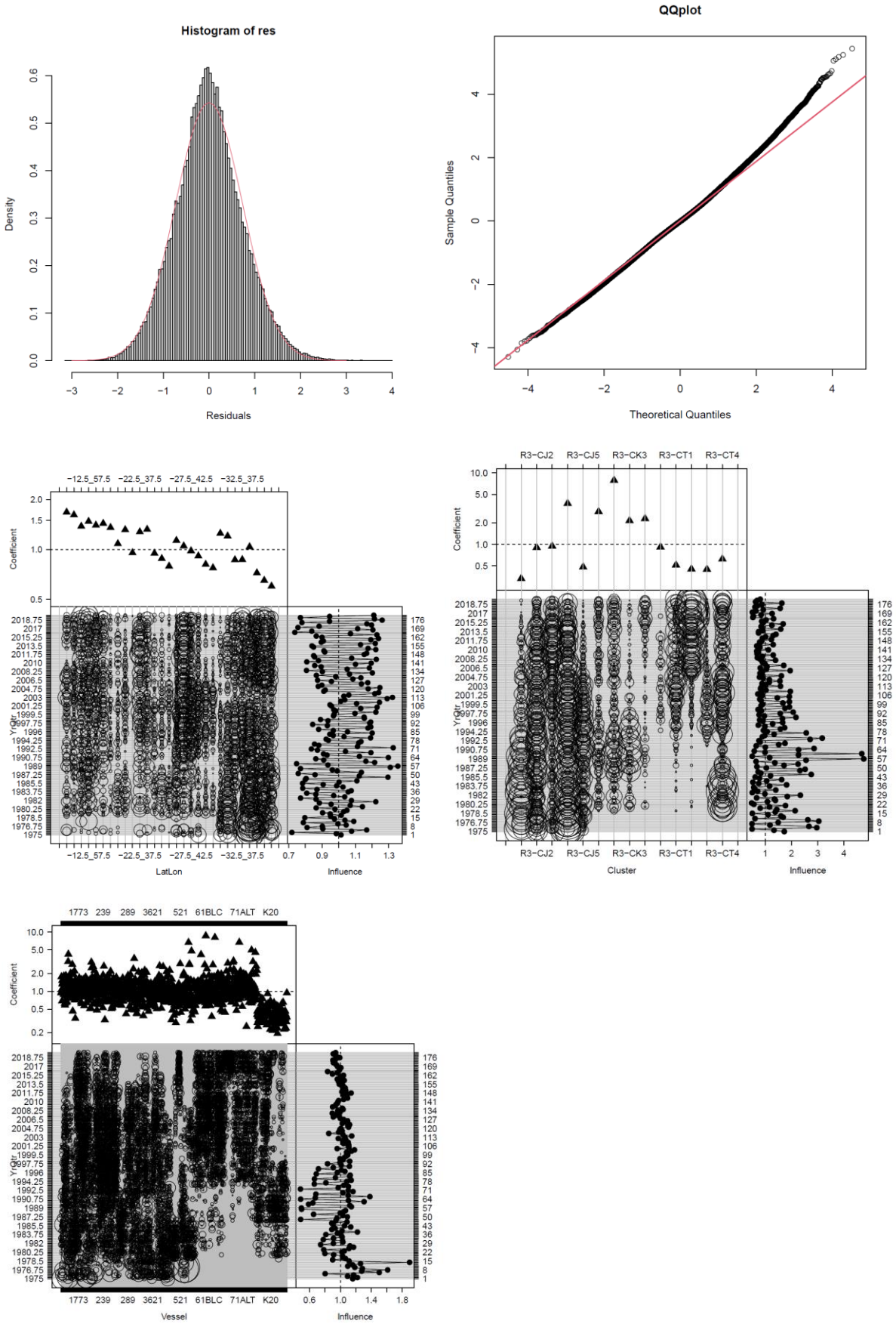

Figure 9(a): Diagnostics and influence plots for LN(~ YrQ + LonLat + Cluster+Vessel) for R3.

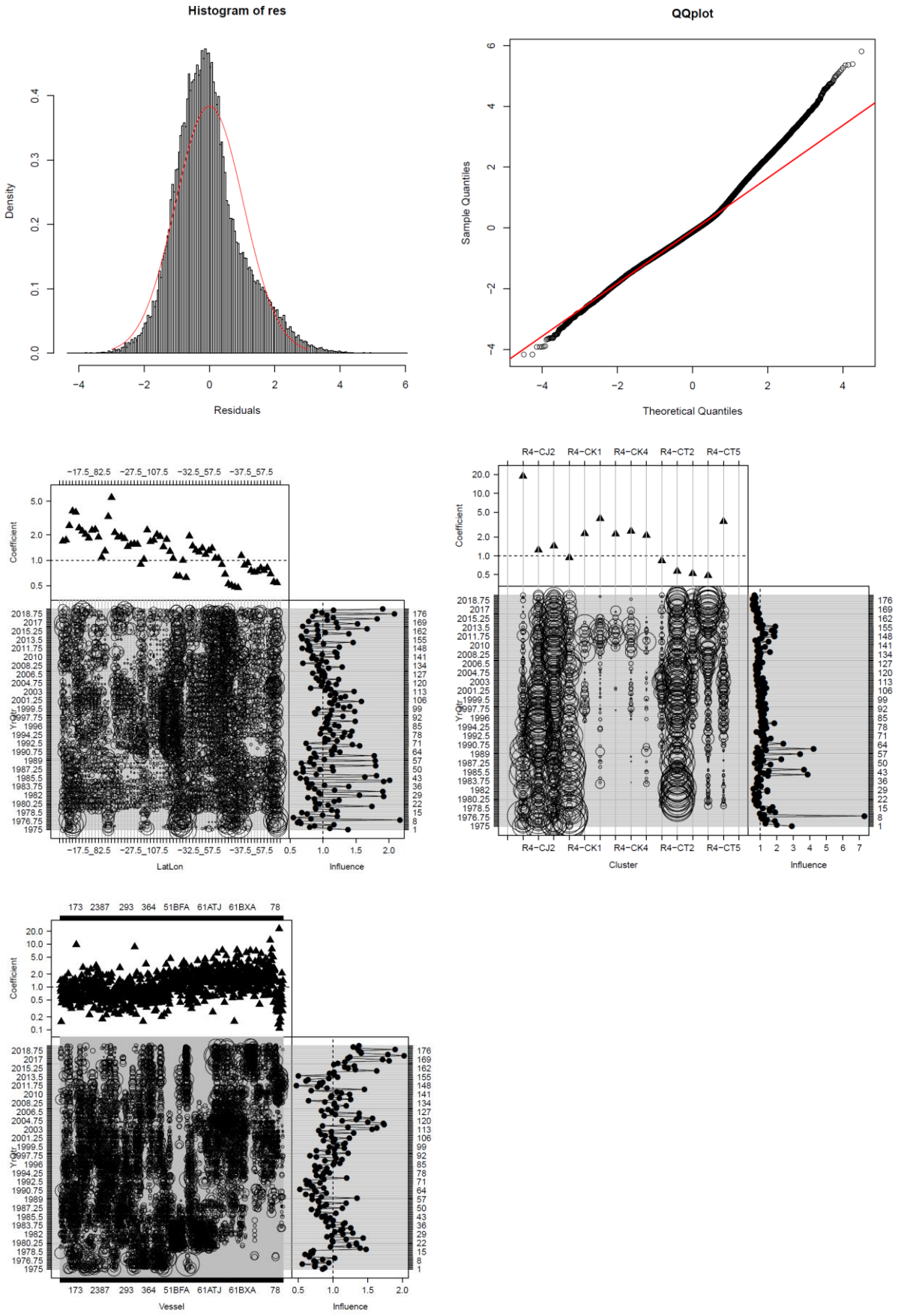

Figure 9(d): Diagnostics and influence plots for LN(~ YrQ + LonLat + Cluster+Vessel) for R4. (see Table 10, too)

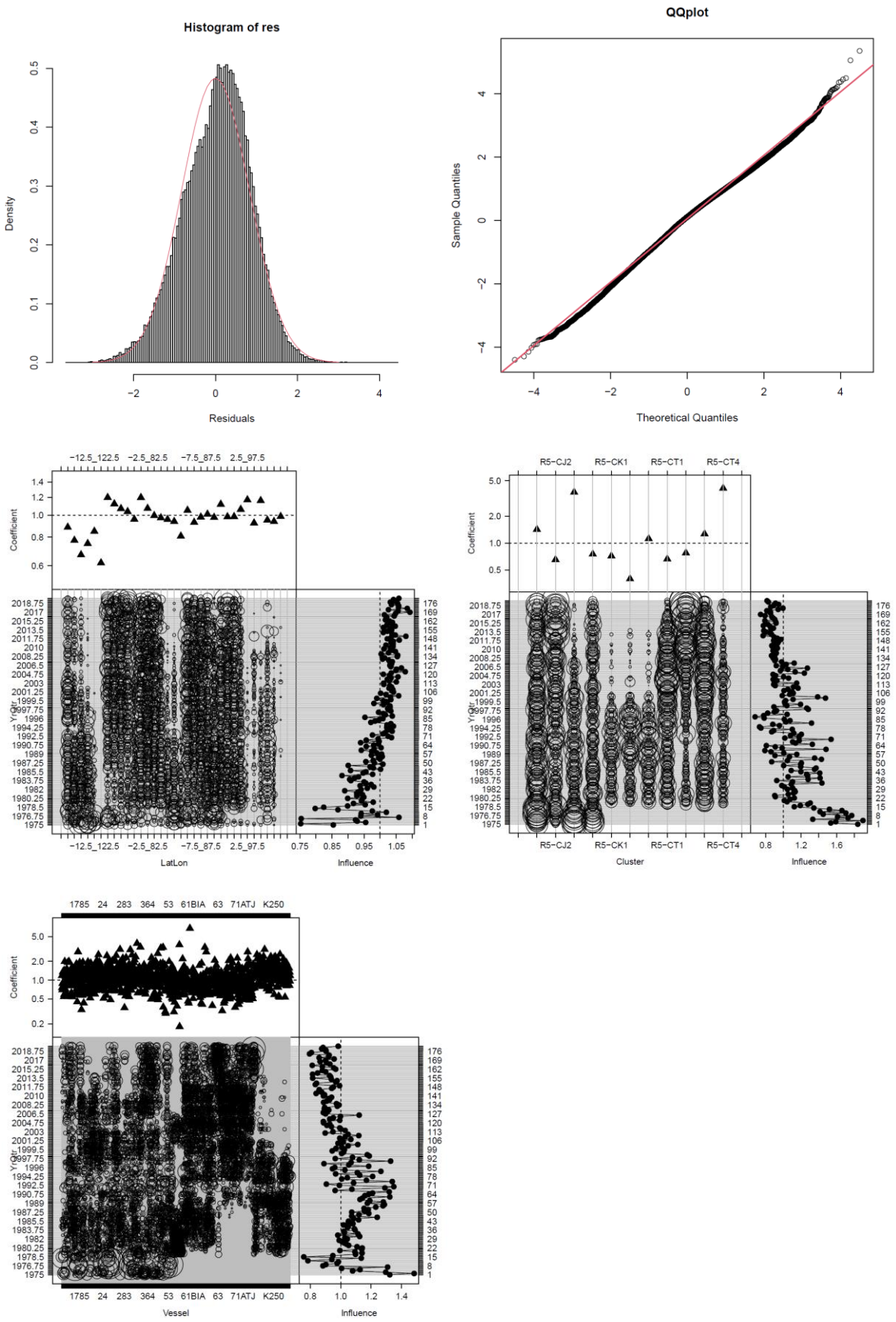

Figure 9(e): Diagnostics and influence plots for LN(~ YrQ + LonLat + Cluster+Vessel) for R5.

(Residual plots for the positive component)

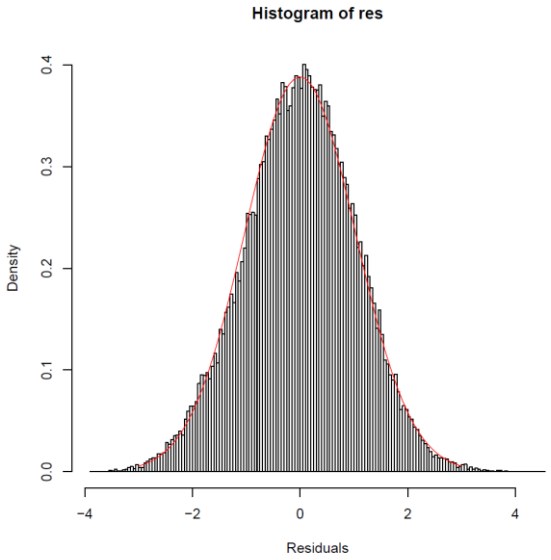

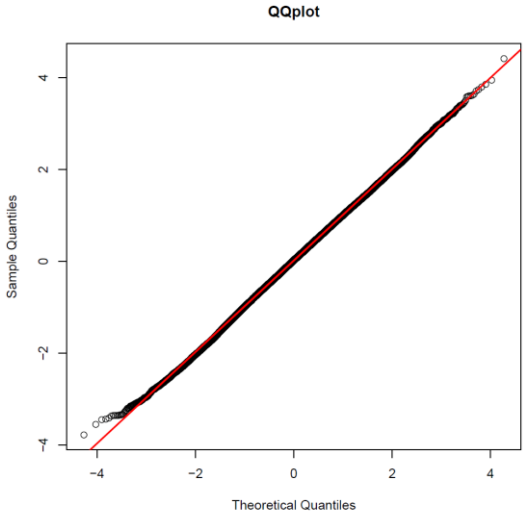

(Influence plots for the delta component)

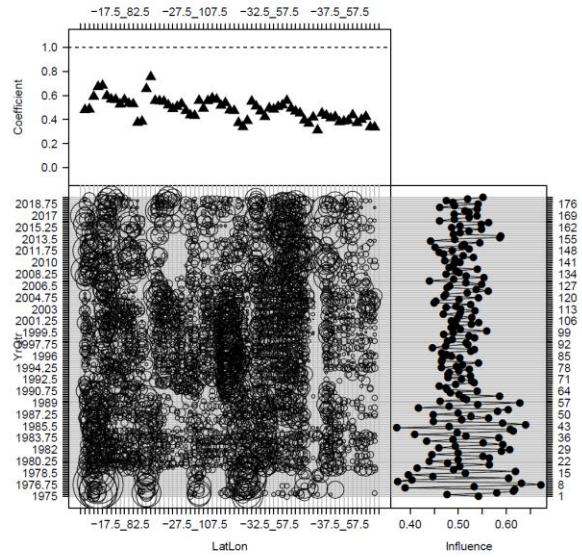

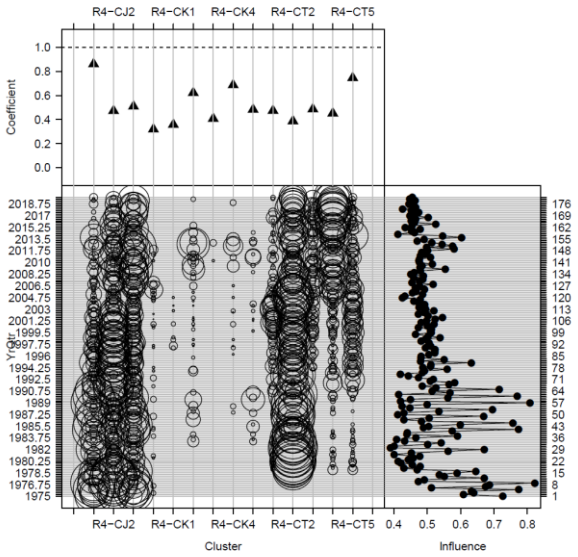

(Influence plots for the positive component)

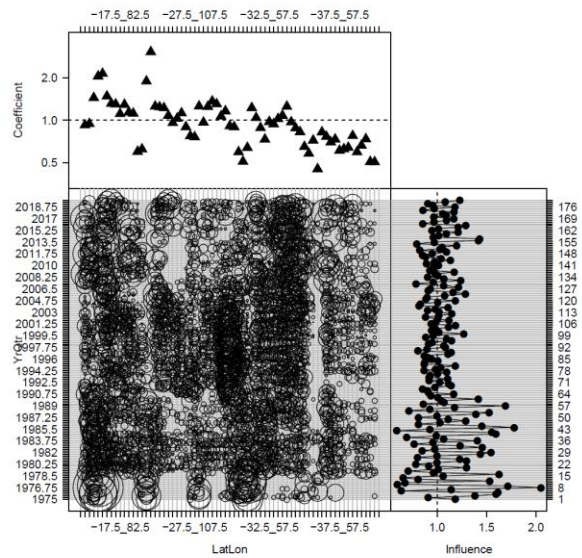

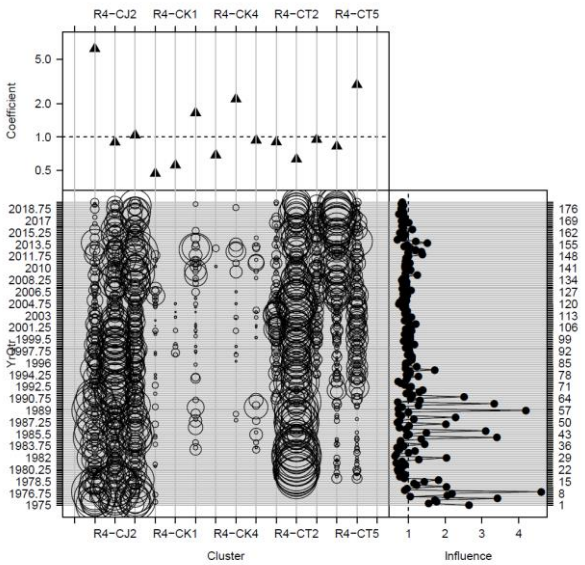

Figure 10: Diagnostics and influence plots for the DL model with D(~ YrQ + LonLat + Cluster) & LN(~ YrQ + LonLat + Cluster) for R4.